Diatom responses and geochemical feedbacks to environmental changes at Lake Rauchuagytgyn (Far East Russian Arctic)

Boris K. Biskaborn[1], Amy Forster[1,2], Gregor Pfalz[1,3], Lyudmila A. Pestryakova[4], Kathleen Stoof-Leichsenring[1], Jens Strauss[5], Tim Kröger[1,6], Ulrike Herzschuh[1,2,7]

[1]Alfred Wegener Institute Helmholtz Centre for Polar and Marine Research, Polar Terrestrial Environmental Systems, Telegrafenberg A45, 14473 Potsdam, Germany
[2]University of Potsdam, Institute for Biochemistry and Biology, 14469 Potsdam, Germany
[3]University of Potsdam, Institute of Geosciences, 14469 Potsdam, Germany
[4]North-Eastern Federal University of Yakutsk, 677000 Sakha Republic, Russia
[5]Alfred Wegener Institute Helmholtz Centre for Polar and Marine Research, Permafrost Research, 14473 Potsdam, Germany
[6]Technische Universität Berlin, 10623 Berlin, Germany
[7]University of Potsdam, Institute of Environmental Science and Geography, 14469 Potsdam, Germany

Correspondence to: Boris K. Biskaborn (boris.biskaborn@awi.de)

Abstract. This study is based on multiproxy data gained from a ^{14}C-dated 6.5 m long sediment core and a ^{210}Pb-dated 23 cm short core retrieved from Lake Rauchuagytgyn in Chukotka, Arctic Russia. The main objectives are to reconstruct the environmental history and ecological development of the lake during the last 29k years and to investigate the main drivers behind bioproduction shifts. The methods comprise age-modeling and accumulation rate estimation, light-microscope diatom species analysis (74 samples), organic carbon, nitrogen, and mercury analysis. Diatoms have appeared in the lake since 21.8 cal ka BP and are dominated by planktonic *Lindavia ocellata* and *L. cyclopuncta*. Around the Pleistocene-Holocene boundary, other taxa including planktonic *Aulacoseira* and benthic fragilarioid (*Staurosira*) and achnanthoid species increase in their abundance. There is strong correlation between variations of diatom valve accumulation rates (DAR, mean 176.1 10^9 valves m^2 a^1), organic carbon accumulation rates (OCAR, mean 4.6 g m^{-2} a^{-1}), and mercury accumulation rates (HgAR, mean 63.4 μg m^{-2} a^{-1}). We discuss the environmental forcings behind shifts in diatom species and found responses of key-taxa to the cold glacial period, postglacial warming, Younger Dryas, and the Holocene Thermal Maximum. The short core data likely suggest recent change of the diatom community at 1907 CE related to human-induced environmental change. Significant correlation between DAR and OCAR in the Holocene interglacial indicates within-lake bioproduction as the main source of carbon deposited in the lake sediment. During both glacial and interglacial episodes HgAR is mainly bound to organic matter in the lake associated to biochemical substrate conditions. There were only ambiguous signs of increased HgAR during the industrialization period. We conclude that pristine Arctic lake systems can serve as CO_2 and Hg sinks during warming climate driven by insolation-enhanced within-lake primary productivity. Maintaining intact natural lake ecosystems should therefore be of interest to future environmental policy.

1 Introduction

Today, northern and mountain regions warm faster than elsewhere on Earth, putting cold freshwater systems at risk for loss of ecosystem services (Ipcc, 2021). Paleoenvironmental research, however, still lack sufficient geographical coverage in the eastern Russian Arctic (Kaufman et al., 2020; Mckay et al., 2018; Sundqvist et al.,

2014). Arctic lakes are powerful archives of past climate information because they respond rapidly to external forcing on their catchments (Biskaborn et al., 2021b; Nazarova et al., 2021; Subetto et al., 2017). Effects of both, past climate changes and modern human impacts during the industrial period, including mercury contamination of pristine ecosystems have been demonstrated for remote Siberian lake ecosystems (Biskaborn et al., 2021a). In paleolimnological research many studies are based on concentrations of fossil remains and geochemical compounds in the sediments. Within the eastern Arctic, yet only few studies managed to accomplish reconstruction of accumulation rates of these sediment constituents, possibly owed to limited age-controls (Vyse et al., 2021).

The Pleistocene-Holocene transition from glacial to interglacial climates commonly reveals the major change within biotic and geochemical sediment components and is well detectable in sufficiently old lake sediments. Shorter and less powerful climate events are less distinctly represented in low-accumulation systems, and their impacts on lake ecosystems in sparsely covered areas is not yet sufficiently understood (Kaufman et al., 2004; Subetto et al., 2017; Biskaborn et al., 2016; Renssen et al., 2012). One of the most known groups of photosynthetic organisms in Arctic lakes are diatoms (Smol and Stoermer, 2010). They are siliceous microalgae (Bacillariophyceae) that form opaline valves which preserve excellent in lake mud and allow identification up to highest species levels by light microscope analysis (Battarbee et al., 2001). Diatoms as a group are one of the major primary producers in aquatic environments, contributing to the global net primary production at about 25% (Stoermer and Smol 2001). Diatom communities respond to numerous environmental forcings including hydrochemical changes, seasonal climate shifts (duration of ice cover), and physical habitat changes (Hoff et al., 2015; Douglas and Smol, 2010; Pestryakova et al., 2018; Herzschuh et al., 2013; Biskaborn et al., 2012; Biskaborn et al., 2013; Palagushkina et al., 2017). Diatom productivity has been estimated from Si/Al ratios (Vyse et al., 2020), valve concentrations (Biskaborn et al., 2012), and biogenic opal concentrations (Meyer et al., 2022). However, there is yet only sparse information available in the literature addressing the contribution of aquatic bioproduction, i.e. diatom primary producers, to accumulation rates of organic matter over different climate stages (Biskaborn et al., 2021b).

Palaeoenvironmental records that include the last glacial maximum (LGM) are sparse in the vast region of Chukotka (Vyse et al., 2020). Lake archives exceeding the LGM were published for Lake El'gygytgyn (Melles et al., 2007), Lake Ilirney (Vyse et al., 2020; Andreev et al., 2021), and Lake Rauchuagytgyn (Vyse et al., 2021), of which the latter is subject of our study. There is still insufficient knowledge about feedbacks of specific climate events, such as the Younger Dryas cooling (Andreev et al., 2021; Kokorowski et al., 2008) or the Holocene Thermal Maximum (Renssen et al., 2012), to lake primary producers. However, short-term and fast events that could compare to the pace of recent climate change are of specific interest to understand today's climate-ecosystem relationships.

Over the last years influences of past and recent climate changes to diatom assemblage shifts were investigated in lakes records in Yakutia (Kostrova et al., 2021; Courtin et al., 2021; Biskaborn et al., 2021b), accompanied by lake ecosystem feedbacks and long-distance heavy metal contamination (Biskaborn et al., 2021a). This study was accordingly set up to test whether similar palaeolimnological responses to climate and anthropogenic impacts exist in very remote areas in Chukotka. In our paper we present new diatom records and biogeochemical data based on the published chronological sediment records and climate reconstructions of lake Rauchuagytgyn (Andreev et al., 2021; Vyse et al., 2021). Our objectives on Lake Rauchuagytgyn are to (1) reconstruct accumulation of diatoms since the last glacial in comparison to bulk organic carbon accumulation, (2) to investigate the main drivers behind

85   assemblage and bioproduction shifts, and (3) to compare past natural and recent mercury loads to test for potential heavy metal contamination of remote pristine ecosystems.

2 Study Site

The catchment of Lake Rauchuagytgyn (67.82° N, 168.7° E, elevation 625 m a.s.l, surface area 6.1 km^2, maximum water depth 36 m, catchment area 214.5 km^2) is located in the north-western Anadyr Mountains of Chukotka in

90   the northeastern Russian Arctic (Fig. 1). The lake's main inflows are situated at the southern margin and a few outflows drain the lake to the north and the sides. Glacial activity in the catchment is preserved by moraine structures north of the lake and in surrounding glacial cirques (Glushkova, 2011; Vyse et al., 2021). The basement of the study site consists of silicic-intermediate lithology, represented by cretaceous Andesite (Zhuravlev et al., 1999). The area is characterized by strong Arctic continental climate with mean annual air temperatures of -11.8

95   °C, mean July and January temperatures are 13 °C and -30 °C, respectively, while annual precipitation is at ca. 200 mm (Menne et al., 2012). Open herb- and graminoid tundra, with tree-occurrence only in lower elevations and close to rivers, characterizes the surrounding landscape (Huang et al., 2020; Shevtsova et al., 2020).

3 Materials and Methods

3.1 Field work

100   Field work and coring activities at Lake Rauchuagytgyn (Fig. 1) were performed by helicopter expeditions in July 2016 and July 2018. We used a hand-held echo sounder and a UWITEC gravity corer (60 mm) to retrieve short core 16-KP-04-L19B core with 23 cm length in summer 2016 at a 31.0 m deep part of the lake at (N 67.7888, E 168.7380). After a few hours the core was subsampled in 0.5 to 1 cm slices before transport in dark and cool conditions. A longer parallel core from the same site and expedition was analyzed for pollen and radiocarbon-

105   based chronology (Andreev et al., 2021).

In summer 2018 we used an INNOMAR SES-2000 compact parametric sub-bottom profiler to locate the coring location in the southern sub-basin and retrieved a long core (EN18218, ca. 6.5 m) at 29.5 m water depth using a UWITEC Niederreiter 60 mm piston coring system operated on a platform at anchor (N 67.7894, E 168.7335). Coring, processing and sediment-geochemistry of this sediment core was already described by Vyse et al. (2021).

110   ### 3.2 Chronology

For the chronology of long core EN18218, we used the LANDO age-depth modelling approach In the current version (v1.3), LANDO combines the output of five age-depth modelling software (Bacon, Bchron, clam, hamstr, Undatable) in a single interactive computing platform described in Pfalz et al. (2022). The advantage of this approach over a single age-depth model is that the combined model takes multiple age-depth uncertainty ranges

115   into consideration and reduces biases towards overinterpretation. We have updated the published sedimentation rate (SR) values for EN18218 accordingly, based on the same 23 radiocarbon dates in Vyse et al. (2021) shown in Table 1. According to Vyse et al. (2021) we added the same age offset to the data derived from the surface sample (785 ± 31 a BP), which corresponds to 853 ± 31 years when the 2018 CE expedition year is taken into account.

To date the common era over the industrial period in short core 16-KP-04-L19B, freeze-dried sub-samples were analyzed for ^{210}Pb and ^{137}Cs activities by direct gamma assay in the Liverpool University Environmental Radioactivity Laboratory, using Ortec HPGe GWL series well-type coaxial low background intrinsic germanium detectors (Appleby et al., 1986). [210]Pb and ^{137}Cs were measured from its gamma emissions at 46.5 keV and at 662 keV, respectively. Accuracies of used detectors were determined using calibrated standard sources of known activity. The effect of self-absorption of low-energy gamma rays was used for corrections (Appleby et al., 1992).

To model the chronology of the short core, we used the R package "rPlum" (Blaauw et al., 2021) to apply a Bayesian framework to determine the chronology based on ^{210}Pb measurements (Hunter et al., 2022; Aquino-López et al., 2018). We used 18 measurements of supported and unsupported [210]Pb (Table 2) within Plum, while assuming a varying supply of unsupported ^{210}Pb for the model (Figure 2a.2b). We corrected the Plum model by constraining it with the ^{137}Cs peak between 3 and 3.5 cm (Figure 2c), which is attributed to the high point in atomic weapons testing in 1963 (Appleby, 2001; Hunter et al., 2022).

3.3 Biogeochemistry and mercury analysis

To gain information about the productivity in the lake we analyzed total organic carbon (TOC), total carbon (TC) and total nitrogen (TN) from 20 short core samples 16-KP-04-L19B N from 66 samples from the long core samples EN18218. 25 samples below 220 cm in EN18218, however, revealed TN values below the detection limit (0.1 wt%) and are therefore not displayed. TOC and total inorganic carbon (TIC) were detected using a Vario SoliTOC cube elemental analyser (Elementar Analysensysteme GmbH) following combustion at 400 °C for organic carbon, and 900 °C for TIC. The sum of TOC and TIC was used to estimate TC. TN was measured using a rapid MAX N exceed (Elementar Analysensysteme GmbH). The data was used to calculate the TOC/TN ratio, using a factor of 1.167, which is the ratio of the atomic weights of nitrogen (14.007 amu, atomic mass unit) and carbon (12.001 amu) to obtain the atomic ratio TOC/TN$_{atomic}$ following Meyers and Teranes (2002). TOC from EN18218 was used from Vyse et al. (2021) to estimate TOC/TN$_{atomic}$ ratios for the long core.

Total mercury (THg) was analyzed in 20 samples from core 16-KP-04-L19B and 32 samples from core EN18218. We determined the THg in solid material by thermal decomposition, amalgamation and atomic absorption spectrophotometry using a Direct Mercury Analyzer (DMA-80 evo; MLS-MWS GmbH). The solid samples were weight into 1 ml metal boats which are then combusted at about 750°C under a flow of oxygen, and the Hg in the off-gases is trapped as amalgam on a gold sieve. In a subsequent step, Hg is released and its amount is determined by atomic absorption spectroscopy. We used the certified reference material BCR® - 142R (67µg kg^{-1} Hg) as reference material after every 18th measurement and four standards every beginning of a measuring day. The detection limit of the most sensitive cuvette was <0.003 ng Hg. For each sample, we measured THg at least two times and up to four times if the results showed larger variations.

3.4 Diatom analysis

We analyzed diatoms in a total of 54 samples from sediment core EN18218 and 20 samples from surface core 16-KP-04-L19B, taken from 0.5 cm slices. For light-microscopy based species identification we prepared diatom slides following the procedure described in Battarbee et al. (2001). We treated 0.1 g of freeze-dried sample material with hydrogen peroxide (30 %) for up to 5 hours, added hydrochloric acid (10%) to stop the reaction and washed

the sample with purified water before adding between 5-8x10^6 microspheres, according to the density of valves on the test slides, to estimate concentration of diatom valves (DVC). Homogenized sediment suspension was transferred to cover slips placed in Battarbee cups to avoid species fractionation, and mounted to slides using

160   Naphrax. To identify diatoms to the lowest possible taxonomic level we used a Zeiss Axioscope 5 Light microscope with an Axiocam 208 color camera attached, equipped with a Plan-Apochromat 100x/1.4 Oil Ph3 objective at 1000x magnification. We counted more than 300 diatom valves in each sample (Wolfe, 1997) in both sediment cores (mean 351 valves in EN18218; mean 375 valves in 16-KP-04-L19B). Diatom species identification was based on various literature including Hofmann et al. (2011) and Krammer and Lange-Bertalot (1986-1991) as

165   well as online databases (i.e. http://www.algaebase.org). Correct identification of species was supported by images from a scanning electron microscope and for some species with input from the diatom community online platform DIATOM-L (Bahls, 2015). During diatom analysis, valves were distinguished in pristine and non-pristine valves, and chrysophyte cysts were counted but not further identified.

3.5 Data processing and statistics

170   For statistical analysis of downcore proxy data we used the R environment (R Core Team, 2016). Both cores, EN18218 and 16-KP-04-L19B were statistically analyzed following the same procedure.

To create diatom zones along the cores we used the package 'rioja' for constrained incremental sums-of-squares clustering (CONISS) based on Bray-Curtis dissimilarity after log transformation of all count data to downweigh abundant species (Grimm, 1987).

175   We used the 'decorana' function in the package 'vegan' (Oksanen et al., 2020) to apply a detrended correspondence analysis (DCA) on percentage data and calculated gradient length in standard deviation units (SD EN18218 = 2.36; SD 16-KP-04-L19B = 1.25). According to the threshold suggested by Birks (2010) we chose principal component analysis (PCA) to reveal major trends in square-root transformed data based on Euclidean distance. Before PCA, we filtered the species data to exclude rare species, i.e. only species present with ≥ 3% in ≥ 2 samples

180   were included in PCA. The bottom sample at 540 cm was too different from the rest of the more established diatom assemblage and was therefore excluded from the analysis. To downweigh abundant species, filtered data were square-root transformed.

We estimated diatom species richness (alpha diversity) based on Hill's N0, and N2 diversity (Hill, 1973) and performed rarefaction to correct richness estimates for differences of valve counts (Birks et al., 2016) using the

185   'vegan' R package (Oksanen et al., 2020). The minimum base sum of all samples was n=304 for EN18218 and n=333 for 16-KP-04-L19B.

To estimate diatom valve dissolution, we calculated the F index following Ryves et al. (2001), providing a range between 0 and 1 in which 0 is poor and 1 is perfect preservation.

Pearson correlation matrices were generated using the 'cor' function in the R package 'stats'. To highlight

190   significant correlations by p value criterion, a significance test based on the upper tail probability from the pearson correlation coefficients was performed using the function 'cor.mtest' in the R package 'corrplot'. Only correlations that yielded p values <0.05 were considered significant.

The TOC/N$_{atomic}$ ratios were calculated following Meyers and Teranes (2002) using weight ratios of TOC and N multiplied with 1.167. TOC from EN18218 was used from Vyse et al. (2021) to estimate TOC/N ratios for the

195   long core.

To calculate individual accumulation rates, we first multiplied dry bulk densities (DBD in g cm^{-3}) with sedimentation rates (SR in cm a^{-1}) to generate dry mass accumulation rate values (MAR in g cm^{-2} a^{-1}). Since the DBD measurement of the 16-KP-04-L19B surface sample was missing, we extrapolated the value from samples below by constructing a piecewise polynomial in the Bernstein basis using the Python package "scipy" (Virtanen

200   et al., 2020). To determine uncertainty ranges for the individual accumulation rates we propagated the 2σ uncertainty range of SR into the MAR calculations.

Organic carbon accumulation rates (OCARs) were estimated by dividing TOC (wt-%) by a factor of 100, then multiplying with MAR and converting to g m^{-2} a^{-1} units by multiplying it with a factor 10000. We multiplied Hg values with MAR to estimate mercury accumulation rates (HgAR), but then converted HgAR to µg m^{-2} a^{-1} units

205   by multiplying the HgAR values with a factor 10. Diatom accumulation rates (DAR in valves m^{-2} a^{-1}) were estimated following Birks (2010) by using MAR multiplied with the diatom valve concentration (valves g^{-1}) and concerting it to 10^9 valves m^{-2} a^{-1} units.

Mean summer insolation was calculated for Rauchuagytgyn at (90° from vernal point, 67.8° N, 1365 solar constant) using QAnalySeries 1.5.1 and Earth's orbital parameters from Laskar et al. (2004). Pollen-reconstructed

210   July temperatures (TJuly$_{pollen}$), and annual precipitation (APP$_{pollen}$) from Andreev et al. (2021) were resampled onto the core depths based on their published ages and our age-model output from EN18218. Mean July temperatures from the closest weather station OSTROVNOE (first observation 1936 CE, 68.12°, 164.17°, ID: RSM00025138, 98 m.a.s.l., 195 km W of Lake Rauchuagytgyn) were estimated from daily values retrieved from NOAA (www.noaa.gov) and resampled onto to sample depths of 16-KP-04-L19B based on the plum age model.

215   **4 Results**

4.1 Chronology

The LANDO age-depth model based on radiocarbon dates for EN18218 (Fig. 3) shows an age range of 28,190 to 29,907 cal yr BP (weighted mean age: 28,950 cal yr BP) at 651.75 cm, which agrees with the age-depth model developed by Vyse et al. (2021) of about 29,000 cal yr BP at core base. The weighted mean sedimentation rates

220   of all LANDO models ranges over the entire core from 0.01 cm yr^{-1} to 0.1 cm yr^{-1}, which means that the maximum value is higher in some regions than previously reported (Vyse et al., 2021) with a maximum of 0.054 cm yr^{-1}. However, both models agree on decreases in mean sedimentation rates below 0.02 cm yr^{-1} around 558-560 cm and 346-358 cm, and increases around 510-519 and 371-374 cm, where LANDO models suggest mean values above 0.065 cm yr^{-1}. Additional decline in mean sedimentation rate is found below 0.02 cm yr^{-1} approximately between

225   224-243 cm. Taking into account the 2σ confidence intervals of all models, the uncertainty for the sediment core ranges from minimum values of 0.002 cm yr^{-1} at 569 cm to maximum values of 0.575 cm yr^{-1} between 52-54 cm. The Plum age-depth model based on lead and cesium dates for short core 16-KP-04-L19B (Fig. 4) reaches a maximum mean age of 1864 CE (uncertainty range: 1813 – 1905 CE) at 11 cm. Total ^{210}Pb activity reached equilibrium with the supporting ^{226}Ra at a depth of around 7 cm (Fig. 2), which explains the larger uncertainty

230   between 7 and 11 cm (Fig. 4). Unsupported ^{210}Pb concentrations vary irregularly with depth with significant non-monotonic features between 1-2.5 cm and 3-4.5 cm. Mean sedimentation rates range between 0.03 cm yr^{-1} (2-3 cm) and 0.139 cm yr^{-1} (0-1 cm), where the higher values can be explained by the lack of ^{210}Pb data for the first

Diatoms occurred upward of 541cm (21.8 cal ka BP) in long core EN18218 (Fig. 5) and were found in all samples between 0 and 10.5 cm counted from short core 16-KP-04-L19B (Fig. 6). In total 204 different species were identified. The dominant taxa in the observed samples are represented by planktonic cyclotelloid species, *Aulacoseira* and small achnanthoid species. Chrysophyte cysts only occurred with few counts in two samples (251 and 311 cm in EN18218) and were therefore neglected. The valve dissolution *F* index in both long (min. 0.78, max. 0.95, mean 0.90) and short core (min. 0.86, max. 0.98, mean 0.94) was generally high referring to an overall good valve preservation.

Mean diatom valve concentrations (DVC) in EN18218 were 46.4 (2.3-134.7) 10^7 valves g^1, corresponding to diatom valve accumulation rates (DAR) of 176.1 (2.0-651.6) 10^9 valves m^2 a^1. Modern DVC in the short core had a relatively higher mean of 82.0 (43.8-200.4) 10^7 valves g^1, corresponding to DAR of 199.2 (42.2-514.9) 10^9 valves m^2 a^1.

Rarefied species richness Hill's N0 varied between 11.8 and 42.2 (mean 29.4) in the long core and was slightly higher between 31.1 and 47.4 (mean 38.8) in the short core. The effective richness Hill's N2 ranged between 1.5 and 8.4 (mean 3.1) in the long and between 2.9 and 6.1 (mean 4.3) in the short core. A remarkable shift toward high effective richness is found in the long core between ca. 241 and 346 cm.

The first three directions in the principal component analysis explain ca. half of the data variance in EN18218, i.e. PC1, PC2, and PC3 explained 23.2, 17.8, and 11.8 %, respectively. The first three PCA axes from the short core assemblage data explained ca. two third of the data variance, i.e. 28.9, 22.8, and 14.4 % for PC1, PC2, and PC3, respectively. PC3, however, was not included in the biplots shown in Fig. 7.

According to our cluster analysis we divided the cores into 7 diatom zones A-G in core EN18218 and 3 zones H-J in the surface core 16-KP-04-L19B and described the species in chronological order.

Diatom Zone A 541-505 cm (EN18218, 21.8-20.2 cal ka BP)

The oldest diatoms found in the core were dominated by planktonic *Lindavia ocellata* (~57.7%), *Lindavia cyclopuncta* (~26.2%) and *Lindavia bodanica* (~3.1%), accompanied by benthic *Achnanthidium minutissimum*, *Encyonema minutum* and *Nitzschia palea* with lesser abundance.

Diatom Zone B 505-426 cm (EN18218, 20.2-15.3 cal ka BP)

Zone B was dominated by *L. cyclopuncta* (~49.7%), *L. ocellata* (~33.6%), and, appearing in two samples only, *Aulacoseira valida* (~2.5%). *Pliocaenicus costatus* occurred frequent at 441 cm (7.9 %). Benthic species *Staurosira construens*, *Encyonopsis descriptiformis*, *Psammothidium chlidanos* and *Hannaea arcus* appeared with low abundance in addition to the benthic species found in zone A.

Diatom Zone C 426-366 cm (EN18218, 15.3-12.8 cal ka BP)

Dominant planktonic species were represented by *L. ocellata* (~44.1%), *L. cyclopuncta* (~32.4%) and *P. costatus* (~4.9%). *Staurosira pinnata* and *Staurosira brevistriata* occurred in addition to the benthic species found in zone B.

275 *Diatom Zone D 366-346 cm (EN18218, 12.8-11.4 cal ka BP)*

Zone D appeared as a small section (two samples) in which only L. ocellata remained frequent (~61.6%), while other planktonic forms were restricted to first-time occurrence of *Aulacoseira subarctica* (~4.5%) and less frequent *P. costatus*. *Brachysira neoexilis* (~4.1%) started to occur while *S. pinnata* started to became more frequent (~3.0%).

280

Diatom Zone E 346-241 cm (EN18218, 11.4-8.0 cal ka BP)

In the Early Holocene part of the core dominant planktonic species were *L. cyclopuncta* (~37.7%) and *L. ocellata* (~14.8%), accompanied by generally more frequent benthic forms represented by *S. pinnata* (~7.9%), *B. neoexilis* (~6.8%), and *A. minutissimum* (~3.8%).

285

Diatom Zone F 241-166 cm (EN18218, 8.0-5.3 cal ka BP)

Zone F started with the dominance of *L. cyclopuncta* (~57.7%), while other *Lindavia* species disappeared. Instead, *A. subarctica* (~4.8%), *P. costatus* (~3.2%) and *A. valida* (~2.9%) occurred in higher frequencies. *S. pinnata* reached highest values (~8.4%) while *P. chlidanos* and *H. arcus* also showed peaking values.

290

Diatom Zone G 166-11 cm (EN18218, 5.3-1.1 cal ka BP)

The upper part of long core EN18218 was characterized by the re-occurrence of *L. ocellata* (~15.0%) and strong representation of *A. subarctica* (~9.2%), while *L. cyclopuncta* (~53.8%) remained the dominant species. Benthic *Staurosira* forms and *A. minutissimum* decreased.

295

Diatom Zones in the short core H-J 10.5-7.0-1.5-0.5 cm (16-KP-04-L19B, 1870-1907-2003-2012 CE)

The strongest shift within the species assemblage of the short core is found at 7 cm. Overall, *L. cyclopuncta* (~37.3%) and *A. subarctica* (~24.4%) remain the most dominant species. *L. ocellata* appears with highest abundance in zone I, i.e. between 7.5 and 4.5 cm (~17.5%), while the same zone is characterized by high values
300 of benthic *Pinnularia nodosa*.

4.3 Biogeochemical variables

We complemented geochemical data from core EN18218 (Fig. 8) provided by Vyse et al. (2021) for TN and THg measurements. TN varied from >0.1 to 0.25 wt%, with highest values in the upper 100 cm of the core. Resulting TOC/TN$_{atomic}$ ratios ranged between 6.0 and 19.2, with strong increase at 341 cm. THg in the same core ranged
305 between 93.2 and 362.8 µg kg^{-1}, with highest value in the sample at 600.25 cm and overall higher mean values above 321 cm (mean 198.6 compared to 141.8 µg kg^{-1} below). Mean Hg accumulation rates (HgAR) estimated from these concentrations were 63.4 (11.8-138.6) µg m^{-2} a^{-1}. Mean organic carbon accumulation rates (OCAR) estimated from TOC values published by Vyse et al. (2021) were 4.6 (0.8-12.7) g m^{-2} a^{-1}. Low peaks in OCAR,

DAR, and HgAR in both cores correspond to low sedimentation rates at 230, 350, and 550 cm in EN18218, and
310   between 2 and 3 cm in 16-KP-04-L19B (Fig. 3 and 4).

Data from short core 16-KP-04-L19B are presented for the first time (Fig. 6 and 9). TOC ranged between 2.6 and
3.5 wt%, with highest values in the upper 3 cm. N varied between 0.28 and 0.41 wt%, resulting in TOC/TN$_{atomic}$
ratios with only little fluctuation around mean 10.7, which is fitting to the upper part of EN18218. THg in the short
core varied between 162.4 and 244.7 µg kg^{-1}, with highest values in between 4.5 and 3 cm. Mean OCAR and
315   HgAR estimated from TOC and THg concentrations were 6.7 (2.7-11.5) g m^{-2} a^{-1} and 46.0 (14.3-69.8) µg m^{-2} a^{-1},
respectively.

5 Discussion

5.1 Ecological responses of diatom species to Late Quaternary environmental changes

Diatoms in Lake Rauchuagytgyn started to appear at 21.8 cal ka BP (Fig. 5) with strong dominance of *L. ocellata*
320   (Pestryakova et al., 2018), a planktonic and ultraoligotrophic to mesotrophic taxon, common in cold lakes
(Wunsam et al., 1995). The first occurrence of diatoms was accompanied with the first increase of organic carbon
accumulation (Fig. 8). According to previous sedimentological work on the sediment core (Vyse et al., 2021), at
this time glaciers retreated from the catchment and unfrozen episodes became more frequent leading to paraglacial
deposition progressing in the lake basin. In the course of continued deglaciation since ca. 20 cal ka BP in Chukotka
325   (Vyse et al., 2020) and Alaska (Elias and Brigham-Grette, 2013) the diatom assemblage developed progressively
in diatom zones A and B, enabling oligotrophic *L. cyclopuncta* (Scussolini et al., 2011) and few benthic species to
occupy ecological niches in the young and still cold lake ecosystem. Strong fluctuations, e.g. of tychoplanktonic
A. valida, still indicates unstable habitat conditions. *Pliocaenicus costatus* is known in larger quantities from cold
and strongly oligotrophic mountain lakes restricted to East Siberia (Cremer and Van De Vijver, 2006). Limitation
330   of benthic diatoms may result from in-wash of clay during deglaciation (Vyse et al., 2021) leading to low-
transparent and narrow littoral zones in an overall deep basin. In diatom zone C the species richness increased
strongly and benthic diatoms became abundant (Hill's N0, planktonic/benthic ratio in Fig. 8) supporting a gradual
climate amelioration equivalent to the Bølling-Allerød interstadial, which started ca. 15.5-15.0 cal ka BP
(Wohlfarth et al., 2007; Obase and Abe-Ouchi, 2019; Andreev et al., 2021) facilitating shallow water habitats and
335   thus more complex diatom communities due to longer growing seasons (Cherapanova et al., 2007).

The short but remarkable diatom zone D is characterized by the same cold-adapted planktonic and parts of benthic
species from the early deglacial period in diatom zone B. Thus, in accord to other findings from Chukotka
(Anderson and Lozhkin, 2015) and i.e. Lake El'gygytgyn (Andreev et al., 2012), the Rauchuagytgyn diatom
assemblage provides evidence of an aquatic ecosystem response to climate cooling and drying between ca. 12.8-
340   11.4 cal ka BP corresponding to the Younger Dryas.

The Pleistocene/Holocene (P/H) boundary is detected from the diatom assemblage change at ca. 346 cm in core
EN18218, fitting well to the uncertainty range of 10.8-12.2 cal ka BP (Fig. 5 and Fig. 3). At the glacial-interglacial
transition, the diatom community responded with a strong decrease of planktonic and light *Lindavia* species
(Biskaborn et al., 2021b) that was accompanied with a decrease in both diatom and carbon accumulation rates
345   (Fig. 8). Mountain ice-sheets that persisted in the catchment over the deglacial period vanished at the P/H boundary
leading to decreased water supply and lower lake levels over the Early Holocene. At that time, the effective species

richness (Hill's N2) increased because relatively more benthic species reached higher percentages, while the pure richness (N0) slightly decreased. The P/H is also characterized by a clear increase of the first axis sample scores of the PCA (Fig. 8). The PCA biplot depicts grouping of planktonic *Lindavia* versus benthic *Staurosira* and

350 *Psammothidium* species along the primary axis while *Aulacoseira* species are oriented along the secondary axis (Fig. 7). Fragilarioid forms such as *S. pinnata*, *S. construens*, and *S. brevistriata* are known as typical small benthic pioneering forms in boreal shallow lakes (Valiranta et al., 2011; Biskaborn et al., 2012) that are often alkalophilous (Paull et al., 2017). Together with the increase of achnanthoid taxa, this assemblage indicates increased availability of littoral habitats with nearby woody vegetation (Andreev et al., 2021) on fresh soils leading to enhanced ion

355 supply and eventually increased alkalinity to the lake (Herzschuh et al., 2013).

At the P/H transition, abrupt high TOC/TN$_{atomic}$ values of around 15 (Fig. 8) point to a higher contribution of less-degraded organic carbon, indicating an increase of benthic water plants and terrestrial plant material (Meyers and Teranes, 2002; Baird and Middleton, 2004) and thus provides evidence for shallower shores and development of catchment vegetation due to maximal summer insolation and warm interglacial conditions (Fig. 8). The increased

360 role of water plants is supported by epiphytic *B. neoexilis, E. minutum, A. minutissimum* and *E. descriptiformis* (Barinova et al., 2011; Hofmann et al., 2011).

Swann et al. (2010) reconstructed most favorable climate conditions known as the Holocene Thermal Maximum (HTM) at Lake El'gygytgyn (140 km to E) between 11.4 and 7.6 cal ka BP. However, based on pollen data, Andreev et al. (2021) reconstructed the start of warmest conditions at ca. 8.0 cal ka BP for the Rauchuagytgyn

365 region. At 8.0 cal ka BP in diatom zone F, *L. ocellata* disappeared together with low levels of *L. bodanica,* while *Aulacoseira* species started to establish. *Aulacoseira* builds heavy and rapidly sinking frustules commonly found in deep boreal lakes (Laing and Smol, 2003). Euplanktonic *A. subarctica* is a pelagic species that requires turbulence to remain in the photic zone (Rühland et al., 2008; Gibson et al., 2003), while light cyclotelloid taxa prefer stratified water conditions (Rühland et al., 2015). We assume that high July temperatures continued but in

370 addition the open water seasons prolonged around 8-7 cal ka BP, as winters in Siberia gradually became warmer over the mid- and Late Holocene (Meyer et al., 2015). Thus, early ice-out and longer spring circulation supported *Aulacoseira* species (Horn et al., 2011) and led to a drastic change in the Rauchuagytgyn species assemblage. For comparison, in recent times, a surface ice-layer in Chukotka lakes builds up in October reaching up to 1.8 m over the winter, and breaks up in early July after snow melt started in mid-May (Nolan et al., 2002).

375 At ca. 6.4 cal ka BP the DAR, OCAR, TOC/TN$_{atomic}$ ratios increased (Fig. 8), while *L. bodanica* reappeared, *A. valida* increased strongly but small benthic *Staurosira* species retreated (Fig. 5). We interpret this change with maturation of soils (Biskaborn et al., 2012), retreating woody vegetation (Andreev et al., 2021), and a shift in bioproduction driven by increased supply of nutrients through increased river activity and increasing water levels (Buczkó et al., 2013). During the cooling of the Late Holocene the diatom zone G assemblage continuous as a

380 semi-pelagic cold water community at intermediate to high water levels, high DAR but slightly decreased richness and also decreasing terrestrial influence indicated by lowering TOC/TN$_{atomic}$ values.

The last decades are represented in the short core 16-KP-04-L19B about 200 m E of the long core position. These surface sediments were also dominated by the same *Lindavia* and *Aulacoseira* species as compared to diatom zone G (Fig. 9). The main assemblage change occurred at ca. 1907 CE characterized by increases in the benthic taxa

385 *Psammothidium chlidanos* and *Pinnularia nodosa*, accompanied by a slight shift from *Aulacoseira* to *Lindavia* species and decreasing OCAR, DAR, and HgAR, but slightly increased TOC/TN$_{atomic}$ values (Fig. 9). The *Aulacoseira-Lindavia* shift is tentatively supported in the PCA biplot in PC1 (Fig. 7). Even though the overall

response to recent environmental changes in Rauchuagytgyn seems of minor extent, the timing and response corresponds to warming at high latitudes observed during industrialization (Biskaborn et al., 2021a). Abrupt shifts

390   in lake ecosystems were most frequently observed around 1950 CE (Huang et al., 2022) when the beginnings of human energy consumption and geochemical impacts initiated the (proposed) Anthropocene epoch (Syvitski et al., 2020). A strong warming at 1950 CE was also documented in air temperature observations in the weather station 195 km W of the study area. In Rauchuagytgyn, DAR decreased strongly at that time, while HgAR and TOC/TN$_{atomic}$ ratios fluctuated having a negative influence on species richness N0 and N2 (Fig. 9). In between ca.

395   1960 and 1985 CE there is a peak in *Tabellaria flocculosa*, a species that can occur with both planktonic and benthic life styles (Heudre et al., 2021) indicating slightly acidic environmental conditions, and may be responding to unstable habitat conditions (Palagushkina et al., 2012). Since 1990 CE DAR, OCAR and Hg increased again while *A. subarctica* and *P. nodosa* decreased, pointing to either minor atmospheric influences on the lake hydrochemistry, or natural short-term variation (Gibson et al., 2003).

400

5.2 Correlation between carbon, diatoms and mercury accumulation

Accumulation rates (AR) are generally rather uncertain, due to limitations in precise estimation of sedimentation rates from age-model interpolations (Sadler, 1981). In our study this effect is relevant due to the conversion from weight concentrations of organic carbon and mercury to AR through multiplication with sedimentation rates from

405   age modelling and bulk densities related to water contents (Vyse et al., 2021). Diatom concentrations, however, are expressed as numbers of frustules (Battarbee et al., 2001). Accordingly, one cannot directly infer diatom biomass from count-based DAR as taxa vary considerably in size among and within species (Birks, 2010). As discussed above, the diatom succession in the Rauchuagytgyn sedimentary record shows a tendency toward lake ontogeny (Brenner and Escobar, 2009). We thus expect (unknown) changes in the relation between biomass and

410   number of valves that cannot be ruled out. Acknowledging the overall strong bias in AR we still attempt to quantify carbon, diatom, and Hg trajectories to help assessing northern lake systems as freshwater carbon sinks.
At millennial time scale in the long core OCAR is strongly correlated with HgAR (r 0.94, p<0.05) and significantly with DAR (r 0.64, p<0.005), while there is no significant correlation between diversity indices to HgAR (Fig. 10). The mean values at around 11.2 (and 12.9 in the Holocene) of TOC/TN$_{atomic}$ measured in the long core represent

415   a mixture of (in simple words) high-N planktonic algae, medium-N benthic water plants and low-N terrestrial vegetation input (Baird and Middleton, 2004). Phytoplankton produces TOC/TN$_{atomic}$ ratios of 4-10, whereas vascular land plants produce >20 (Meyers and Teranes, 2002). Given the sparse vegetation cover around the lake (Huang et al., 2020) and the overall low TOC/TN$_{atomic}$ ratios terrestrial input may play a minor role. We therefore assume that there is a strong contribution of algae to the bulk organic matter accumulated in the lake which tends

420   to be somewhat proportionate to the number of diatom valves. Accordingly, the TOC/TN$_{atomic}$ ratios correlate negatively with planktonic/benthic ratios in the long core (r -0.57, p<0.05), but only slightly (insignificantly) in the short core (r 0.21, p>0.05). This mismatch could indicate that there is anthropogenic nitrogen contribution from the atmosphere (Biskaborn et al., 2021a) that is in addition masked by short-term fluctuations and constraints of measurement precision in high-resolution samples from lakes under extreme environmental conditions. A

425   tentative relationship between DAR and planktonic species could be detected in the short core (r 0.41, p<0.05)

which could indicated, that the wide spread increase of planktonic species in high-latitude lakes as a response to global warming (Smol et al., 2005) contributes to increased diatom primary productivity.

Over the last centuries visible in the short core there is also a significant correlation between OCAR and HgAR. Atmospheric mercury, however, is not simply deposited in Arctic lakes, but instead there is a strong influence of

430   limnological processes such as primary production and ice cover dynamics on mercury biogeochemical cycling (Korosi et al., 2018). The correlation between OCAR and DAR (r 0.65, p<0.05) apparently shows that diatoms play a role in these processes. In contrast to long time scales there is a significant negative correlation in the short core between HgAR and diversity estimates Hill's N0 (r -0.51, p<0.05) and N2 (r -0.39, p<0.05). Thus, contaminants during the industrial period could be assumed to have a stronger effect on the lake ecosystem than

435   natural Hg supply before increased anthropogenic activity (Huang et al., 2022). Studies on deep permafrost soils in Siberia showed that average Hg concentrations of 9.7 µg kg^{-1} could be used as a baseline for natural Hg concentrations (Rutkowski et al., 2021). However, as Hg binds to lake organic carbon (Braaten et al., 2018), lake bioproductivity is likely increasing the mercury load within sediments, explaining the overall high concentrations in older sections. Furthermore, we found a very good correlation between HgAR and OCAR during the cold glacial

440   period (r 0.98 p<0.05) but obvious decoupling from diatoms as shown by missing correlation between HgAR and DAR (Fig. 10). It can be assumed that other C sources than within-lake bioproduction, such as external supply of organic matter represented the main source of the cold climate carbon deposition.

5.3 Long-term ecosystem feedbacks to climate changes

445   Well-preserved and old diatom records in Chukotka provide the opportunity to study direct responses of natural lake ecosystems to regional climate changes (Cherapanova et al., 2007; Swann et al., 2010). The Lake Rauchuagytgyn sediment record provides insight to compositional changes of diatom assemblages in response to lake and catchment changes. The main changes observed are best represented by shifts within planktonic species and their proportions relative to benthic forms populating emerging habitats. Significant negative correlations were

450   found at millennial time scales between planktonic-benthic ratios and diversity estimates Hill's N0 (r -0.7, p<0.05) and N2 (r -0.53, p<0.05), indicating that long-term diatom diversity in Lake Rauchuagytgyn was closely related to lake ontogeny. The general catchment maturation accompanied by decreases of glacial ice-sheet influence led to initiation of new ecological niches and thus diversification of e.g. epiphytic species (Wilson et al., 2012; Rouillard et al., 2012).

455   Diatom accumulation rates on the other hand, recorded independently from lifestyles, show a clear relationship to lake bioproduction. Relationships between diatoms and organic carbon in lake sediments were also related to species alpha diversity in lake Bolshe Toko (Biskaborn et al., 2021b) and explained as stabilizing effects of well-developed species richness supporting primary biomass production (Marzetz et al., 2017). The correlation found between diatom valve and organic carbon accumulation rates during the interglacial in the Rauchuagytgyn

460   sediment record may support that, during warm episodes, diatoms in high-latitude lakes with relatively small catchments are coupled with the bulk production of biomass (Figure 11). Whether or not diatoms might also be synchronized with catchment production remains unclear but not unlikely. Nevertheless, in Lake Rauchuagytgyn we observed a positive feedback mechanism of the freshwater diatom biomass to long-term climate amelioration and thus an increasing role of Arctic lakes as sink for organic matter (Hughes-Allen et al., 2021; Vyse et al., 2021).

465 Compared to ocean systems, where fertilization projects attempted to force carbon burial by artificial diatom blooms (Yoon et al., 2018), lakes may possess a higher potential to withdraw carbon from the atmosphere because of lower carbon remineralization rates (Mendonça et al., 2017; Sobek et al., 2009). However, this may nowadays be questioned because whole-lake experiments and models suggested possible lagged response of lakes natural resistance to anthropogenic stressors that could cause fast ecosystem switches (Pahl-Wostl, 2003). In turn, these

470 potential alterations could possibly prevent carbon sink feedbacks as observed in the remote and still pristine Rauchuagytgyn system. In this context, the observed positive relationship between sedimentary carbon and mercury suggests potential mitigation feedbacks of contamination stress accompanied by recent climate change. However, impacts of human-driven atmospheric stressors only seem little pronounced in the short core data, which is limiting possibilities to assign natural long-term mechanisms to present day conditions. This is amplified by the

475 fact that northern remote lakes have already passed important ecosystem thresholds and are believed to not represent pristine ecosystems anymore (Smol et al., 2005).

6 Conclusions

Radiocarbon and Pb-210 dated sediment cores from Lake Rauchuagytgyn in the Far-East Russian Arctic provide valuable archives of millennial to decadal scale lake ecosystem responses to regional environmental forcing of the

480 last 22000 years before today. Our main findings based on diatom species, organic carbon and nitrogen, and mercury analyses can be highlighted as follows:

- The Pleistocene diatom species assemblage reflects a planktonic community in a deep and cold lake with short growing seasons. The assemblage becomes more complex during a gradual climate amelioration at

485 ca. 15 cal ka BP, similar to Bølling-Allerød, leading to successive development of benthic habitats. Diatom species temporarily returned to glacial conditions between ca. 12.8-11.4 cal ka BP corresponding to the Younger Dryas.

- The Early Holocene diatom community reflects a shallower lake with increased water plants in larger littoral zones and higher alkalinity that we relate to woody vegetation development in the catchment,

490 supported by high carbon to nitrogen ratios. Gradual increasing *Aulacoseira* taxa indicate that winters became warmer over the mid- and Late Holocene leading to earlier ice-out and longer spring circulation.

- During Late Holocene cooling, small benthic *Staurosira* taxa retreated due to soil maturation and increased water levels facilitating higher abundancy of planktonic *Lindavia* and *Aulacoseira* species.

- The last decades represented in a Pb-210 dated short core only show vague evidence of recent change of

495 the diatom community at 1907 CE, indicated by slight increase of light *Lindavia* and decrease of *Aulacoseira* species, accompanied by shifts in the benthic community. Biogeochemical variables and diatom indices fluctuated strongly around 1950 CE.

- Diatom accumulation rates (DAR) and organic carbon accumulation rates (OCAR) do not correlate during the cold episode, but show significant correlation during the warm interglacial when insolation

500 was higher. The Rauchuagytgyn data suggest that during the Holocene (1) deposition of organic carbon was largely driven by within-lake bioproduction, and that (2) diatoms reflect the activity of the gross primary producers of the lake.

505

- Mercury accumulation rates (HgAR) in the investigated sediments are strongly correlated to OCAR in both cold and warm episodes. As Hg accumulation is bound to organic matter, increased carbon sedimentation during warm climates and suitable biochemical substrate conditions facilitates Hg deposition.

- Pristine boreal lake systems potentially can serve as both CO_2 sinks driven by climate-enhanced within-lake primary productivity, and disposal sites for heavy metal contaminants. Consequently, maintaining intact natural lake ecosystems should receive a high priority in future environmental policy.

510 **Data Availability**

Datasets used in this study will be accessible on PANGAEA close upon publication.

Author contributions

BKB conceived the study, conducted field work, statistical analyses, and wrote the manuscript. AF performed
diatom analysis and counting. GF performed age-depth modelling. LAP, KS-F, and UH coordinated field work
and dating of the short core. JS performed mercury analysis. TK performed correlation with p value adjustment.
520 All authors contributed to generating data, writing and review of the manuscript.

Competing interests

The authors declare no conflict of interests.

References

Anderson, P. M. and Lozhkin, A. V.: Late Quaternary vegetation of Chukotka (Northeast Russia), implications for Glacial and
525 Holocene environments of Beringia, Quat. Sci. Rev., 107, 112-128, 10.1016/j.quascirev.2014.10.016, 2015.

Andreev, A. A., Morozova, E., Fedorov, G., Schirrmeister, L., Bobrov, A. A., Kienast, F., and Schwamborn, G.: Vegetation
history of central Chukotka deduced from permafrost paleoenvironmental records of the El'gygytgyn Impact Crater, Clim. Past,
8, 1287-1300, 10.5194/cp-8-1287-2012, 2012.

Andreev, A. A., Raschke, E., Biskaborn, B. K., Vyse, S. A., Courtin, J., Böhmer, T., Stoof-Leichsenring, K., Kruse, S.,
530 Pestryakova, L. A., and Herzschuh, U.: Late Pleistocene to Holocene vegetation and climate changes in northwestern Chukotka
(Far East Russia) deduced from lakes Ilirney and Rauchuagytgyn pollen records, Boreas, n/a,
https://doi.org/10.1111/bor.12521, 2021.

Appleby, P. G.: Chronostratigraphic Techniques in Recent Sediments, in: Tracking Environmental Change Using Lake
Sediments: Basin Analysis, Coring, and Chronological Techniques, edited by: Last, W. M., and Smol, J. P., Springer
535 Netherlands, Dordrecht, 171-203, 10.1007/0-306-47669-X_9, 2001.

Appleby, P. G., Richardson, N., and Nolan, P. J.: Self-absorption corrections for well-type germanium detectors, Nucl. Instrum. Methods Phys. Res., Sect. B, 71, 228-233, https://doi.org/10.1016/0168-583X(92)95328-O, 1992.

Appleby, P. G., Nolan, P. J., Gifford, D. W., Godfrey, M. J., Oldfield, F., Anderson, N. J., and Battarbee, R. W.: 210Pb dating by low background gamma counting, Hydrobiologia, 143, 21-27, 10.1007/BF00026640, 1986.

540 Aquino-López, M. A., Blaauw, M., Christen, J. A., and Sanderson, N. K.: Bayesian Analysis of 210Pb Dating, Journal of Agricultural, Biological and Environmental Statistics, 23, 317-333, 10.1007/s13253-018-0328-7, 2018.

Bahls, L. L.: The role of amateurs in modern diatom research, Diatom Res, 30, 209-210, 10.1080/0269249X.2014.988293, 2015.

Baird, M. E. and Middleton, J. H.: On relating physical limits to the carbon: nitrogen ratio of unicellular algae and benthic
545 plants, J. Mar. Syst., 49, 169-175, https://doi.org/10.1016/j.jmarsys.2003.10.007, 2004.

Barinova, S., Nevo, E., and Bragina, T.: Ecological assessment of wetland ecosystems of northern Kazakhstan on the basis of hydrochemistry and algal biodiversity, Acta Bot. Croat., 70 (2), 215–244, 10.2478/v10184-010-0020-7, 2011.

Battarbee, R. W., Jones, V. J., Flower, R. J., Cameron, N. G., Bennion, H., Carvalho, L., and Juggins, S.: Diatoms, in: Tracking Environmental Change Using Lake Sediments, vol. 3. Terrestrial, Algal, and Siliceous Indicators, edited by: Smol, J. P., Birks,
550 H. J. B., and Last, W. M., Kluwer Academic Publishers, Dordrecht, Netherlands, 155–202, 2001.

Birks, H. J. B.: Numerical methods for the analysis of diatom assemblage data, in: The Diatoms: Applications for the Environmental and Earth Science, edited by: Smol, J. P., and Stoermer, E. F., Cambridge University Press, Cambridge, 23-54, 2010.

Biskaborn, B., Herzschuh, U., Bolshiyanov, D., Savelieva, L., Zibulski, R., and Diekmann, B.: Late Holocene thermokarst
555 variability inferred from diatoms in a lake sediment record from the Lena Delta, Siberian Arctic, J. Paleolimnol., 49, 155-170, 10.1007/s10933-012-9650-1, 2013.

Biskaborn, B. K., Herzschuh, U., Bolshiyanov, D., Savelieva, L., and Diekmann, B.: Environmental variability in northeastern Siberia during the last similar to 13,300 yr inferred from lake diatoms and sediment-geochemical parameters, Palaeogeog. Palaeoclimatol. Palaeoecol., 329, 22-36, 10.1016/j.palaeo.2012.02.003, 2012.

560 Biskaborn, B. K., Narancic, B., Stoof-Leichsenring, K. R., Pestryakova, L. A., Appleby, P. G., Piliposian, G. T., and Diekmann, B.: Effects of climate change and industrialization on Lake Bolshoe Toko, eastern Siberia, J. Paleolimnol., 65, 335-352, 10.1007/s10933-021-00175-z, 2021a.

Biskaborn, B. K., Nazarova, L., Kröger, T., Pestryakova, L. A., Syrykh, L., Pfalz, G., Herzschuh, U., and Diekmann, B.: Late Quaternary Climate Reconstruction and Lead-Lag Relationships of Biotic and Sediment-Geochemical Indicators at Lake
565 Bolshoe Toko, Siberia, Frontiers in Earth Science, 9, 10.3389/feart.2021.737353, 2021b.

Biskaborn, B. K., Subetto, D. A., Savelieva, L. A., Vakhrameeva, P. S., Hansche, A., Herzschuh, U., Klemm, J., Heinecke, L., Pestryakova, L. A., Meyer, H., Kuhn, G., and Diekmann, B.: Late Quaternary vegetation and lake system dynamics in north-eastern Siberia: Implications for seasonal climate variability, Quat. Sci. Rev., 147, 406-421, 10.1016/j.quascirev.2015.08.014, 2016.

570 Blaauw, M., Christen, J., and Aquino-Lopez, M.: rplum: Bayesian Age-Depth Modelling of Cores Dated by Pb-210. R package version 0.2. 2, 2021.

Braaten, H. F. V., de Wit, H. A., Larssen, T., and Poste, A. E.: Mercury in fish from Norwegian lakes: The complex influence of aqueous organic carbon, Sci. Tot. Environ., 627, 341-348, https://doi.org/10.1016/j.scitotenv.2018.01.252, 2018.

Brenner, M. and Escobar, J.: Ontogeny of Aquatic Ecosystems, in: Encyclopedia of Inland Waters, edited by: Likens, G. E.,
575 Academic Press, Oxford, 456-461, https://doi.org/10.1016/B978-012370626-3.00205-2, 2009.

Buczkó, K., Magyari, E. K., Braun, M., and Bálint, M.: Diatom-inferred lateglacial and Holocene climatic variability in the South Carpathian Mountains (Romania), Quat. Int., 293, 123-135, https://doi.org/10.1016/j.quaint.2012.04.042, 2013.

Cherapanova, M., Snyder, J., and Brigham-Grette, J.: Diatom stratigraphy of the last 250 ka at Lake El'gygytgyn, northeast Siberia, J. Paleolimnol., 37, 155-162, DOI 10.1007/s10933-006-9019-4, 2007.

580 Courtin, J., Andreev, A. A., Raschke, E., Bala, S., Biskaborn, B. K., Liu, S., Zimmermann, H., Diekmann, B., Stoof-Leichsenring, K. R., Pestryakova, L. A., and Herzschuh, U.: Vegetation Changes in Southeastern Siberia During the Late Pleistocene and the Holocene, Frontiers in Ecology and Evolution, 9, 10.3389/fevo.2021.625096, 2021.

Cremer, H. and Van de Vijver, B.: On Pliocaenicus costatus (Bacillariophyceae) in Lake El'gygytgyn, East Siberian, Eur. J. Phycol., 41, 169-178, 10.1080/09670260600621932, 2006.

585 Douglas, M. S. V. and Smol, J. P.: Freshwater Diatoms as Indicators of Environmental Change in the High Arctic, in: The Diatoms: Application for the Environmental and Earth Sciences, edited by: Smol, J. P., and Stoermer, E. F., Cambridge University Press, Cambridge, 249-266, 2010.

Elias, S. and Brigham-Grette, J.: Late Pleistocene glacial events in Beringia, Encyclopedia of quaternary science, 2, 191-201, 2013.

590 Esri, D. and GeoEye, E. G.: CNES/Airbus DS, USDA, USGS, AeroGRID, IGN, the GIS User Community, Imagery [basemap]. Scale Not Given."World Imagery, 2019.

Gibson, C. E., Anderson, N. J., and Haworth, E. Y.: *Aulacoseira subarctica*: taxonomy, physiology, ecology and palaeoecology, Eur. J. Phycol., 38, 83-101, 10.1080/0967026031000094102, 2003.

Glushkova, O. Y.: Chapter 63 - Late Pleistocene Glaciations in North-East Asia, in: Developments in Quaternary Sciences, 595 edited by: Ehlers, J., Gibbard, P. L., and Hughes, P. D., Elsevier, 865-875, https://doi.org/10.1016/B978-0-444-53447-7.00063-5, 2011.

Grimm, E. C.: Coniss - a Fortran-77 Program for Stratigraphically Constrained Cluster-Analysis by the Method of Incremental Sum of Squares, Comput. Geosci., 13, 13-35, 1987.

Herzschuh, U., Pestryakova, L. A., Savelieva, L. A., Heinecke, L., Böhmer, T., Biskaborn, B., Andreev, A., Ramisch, A., 600 Shinneman, A. L. C., and Birks, H. J. B.: Siberian larch forests and the ion content of thaw lakes form a geochemically functional entity, Nat. Commun., 4, DOI: 10.1038/ncomms3408, 2013.

Heudre, D., Wetzel, E. C., Lange-Bertalot, H., Van de Vijver, B., Moreau, L., and Ector, L.: A review of Tabellaria species from freshwater environments in Europe, Fottea, 21, 180-205, 10.5507/fot.2021.005, 2021.

Hoff, U., Biskaborn, B. K., Dirksen, V. G., Dirksen, O., Kuhn, G., Meyer, H., Nazarova, L., Roth, A., and Diekmann, B.: 605 Holocene environment of Central Kamchatka, Russia: Implications from a multi-proxy record of Two-Yurts Lake, Global Planet. Change, 134, 101-117, 10.1016/j.gloplacha.2015.07.011, 2015.

Hofmann, G., Lange-Bertalot, H., and Werum, M., Lange-Bertalot, H. (Ed.): Diatomeen im Süßwasser - Benthos von Mitteleuropa, Ganter Verlag, 908 pp.2011.

Horn, H., Paul, L., Horn, W., and Petzoldt, T.: Long-term trends in the diatom composition of the spring bloom of a German 610 reservoir: is Aulacoseira subarctica favoured by warm winters?, Freshwat. Biol., 56, 2483-2499, https://doi.org/10.1111/j.1365-2427.2011.02674.x, 2011.

Huang, S., Zhang, K., Lin, Q., Liu, J., and Shen, J.: Abrupt ecological shifts of lakes during the Anthropocene, Earth-Sci. Rev., 227, 103981, https://doi.org/10.1016/j.earscirev.2022.103981, 2022.

Huang, S., Herzschuh, U., Pestryakova, L. A., Zimmermann, H. H., Davydova, P., Biskaborn, B. K., Shevtsova, I., and Stoof-615 Leichsenring, K. R.: Genetic and morphologic determination of diatom community composition in surface sediments from glacial and thermokarst lakes in the Siberian Arctic, J. Paleolimnol., 64, 225–242, 10.1007/s10933-020-00133-1, 2020.

Hughes-Allen, L., Bouchard, F., Hatté, C., Meyer, H., Pestryakova, L. A., Diekmann, B., Subetto, D. A., and Biskaborn, B. K.: 14,000-year Carbon Accumulation Dynamics in a Siberian Lake Reveal Catchment and Lake Productivity Changes, Frontiers in Earth Science, 9, 10.3389/feart.2021.710257, 2021.

620 Hunter, H. N., Gowing, C. J. B., Marriott, A. L., Lacey, J. H., Dowell, S., and Watts, M. J.: Developments in Pb-210 methodologies to provide chronologies for environmental change, Environ. Geochem. Health, 10.1007/s10653-022-01215-x, 2022.

IPCC: Global Warming of 1.5 C—Climate Change 2021: The Physical Science Basis. Contribution of Working Group I to the Sixth Assessment Report of the Intergovernmental Panel on Climate Change, Cambridge University Press: Cambridge, 625 UK2021.

Kaufman, D., McKay, N., Routson, C., Erb, M., Davis, B., Heiri, O., Jaccard, S., Tierney, J., Dätwyler, C., Axford, Y., Brussel, T., Cartapanis, O., Chase, B., Dawson, A., de Vernal, A., Engels, S., Jonkers, L., Marsicek, J., Moffa-Sánchez, P., Morrill, C., Orsi, A., Rehfeld, K., Saunders, K., Sommer, P. S., Thomas, E., Tonello, M., Tóth, M., Vachula, R., Andreev, A., Bertrand, S., Biskaborn, B., Bringué, M., Brooks, S., Caniupán, M., Chevalier, M., Cwynar, L., Emile-Geay, J., Fegyveresi, J., Feurdean, 630 A., Finsinger, W., Fortin, M.-C., Foster, L., Fox, M., Gajewski, K., Grosjean, M., Hausmann, S., Heinrichs, M., Holmes, N.,

Ilyashuk, B., Ilyashuk, E., Juggins, S., Khider, D., Koinig, K., Langdon, P., Larocque-Tobler, I., Li, J., Lotter, A., Luoto, T., Mackay, A., Magyari, E., Malevich, S., Mark, B., Massaferro, J., Montade, V., Nazarova, L., Novenko, E., Pařil, P., Pearson, E., Peros, M., Pienitz, R., Płóciennik, M., Porinchu, D., Potito, A., Rees, A., Reinemann, S., Roberts, S., Rolland, N., Salonen, S., Self, A., Seppä, H., Shala, S., St-Jacques, J.-M., Stenni, B., Syrykh, L., Tarrats, P., Taylor, K., van den Bos, V., Velle, G.,
635   Wahl, E., Walker, I., Wilmshurst, J., Zhang, E., and Zhilich, S.: A global database of Holocene paleotemperature records, Scientific Data, 7, 115, 10.1038/s41597-020-0445-3, 2020.

Kaufman, D. S., Ager, T. A., Anderson, N. J., Anderson, P. M., Andrews, J. T., Bartlein, P. J., Brubaker, L. B., Coats, L. L., Cwynar, L. C., Duvall, M. L., Dyke, A. S., Edwards, M. E., Eisner, W. R., Gajewski, K., Geirsdottir, A., Hu, F. S., Jennings, A. E., Kaplan, M. R., Kerwin, M. N., Lozhkin, A. V., MacDonald, G. M., Miller, G. H., Mock, C. J., Oswald, W. W., Otto-
640   Bliesner, B. L., Porinchu, D. F., Ruhland, K., Smol, J. P., Steig, E. J., and Wolfe, B. B.: Holocene thermal maximum in the western Arctic (0-180 degrees W), Quat. Sci. Rev., 23, 529-560, 10.1016/j.quascirev.2003.09.007, 2004.

Kokorowski, H. D., Anderson, P. M., Mock, C. J., and Lozhkin, A. V.: A re-evaluation and spatial analysis of evidence for a Younger Dryas climatic reversal in Beringia, Quat. Sci. Rev., 27, 1710-1722, 10.1016/j.quascirev.2008.06.010, 2008.

Korosi, J. B., Griffiths, K., Smol, J. P., and Blais, J. M.: Trends in historical mercury deposition inferred from lake sediment
645   cores across a climate gradient in the Canadian High Arctic, Environ. Pollut., 241, 459-467, https://doi.org/10.1016/j.envpol.2018.05.049, 2018.

Kostrova, S. S., Biskaborn, B. K., Pestryakova, L. A., Fernandoy, F., Lenz, M. M., and Meyer, H.: Climate and environmental changes of the Lateglacial transition and Holocene in northeastern Siberia: Evidence from diatom oxygen isotopes and assemblage composition at Lake Emanda, Quat. Sci. Rev., 259, 106905, https://doi.org/10.1016/j.quascirev.2021.106905,
650   2021.

Krammer, K. and Lange-Bertalot, H.: Bacillariophyceae Band 2/2, Süßwasserflora von Mitteleuropa, 2, Gustav Fischer Verlag, Stuttgart1986-1991.

Laing, T. E. and Smol, J. P.: Late Holocene environmental changes inferred from diatoms in a lake on the western Taimyr Peninsula, northern Russia, J. Paleolimnol., 30, 231-247, 10.1023/a:1025561905506, 2003.

655   Laskar, J., Robutel, P., Joutel, F., Gastineau, M., Correia, A. C. M., and Levrard, B.: A long-term numerical solution for the insolation quantities of the Earth, Astronomy & Astrophysics, 428, 261-285, 10.1051/0004-6361:20041335, 2004.

Marzetz, V., Koussoroplis, A.-M., Martin-Creuzburg, D., Striebel, M., and Wacker, A.: Linking primary producer diversity and food quality effects on herbivores: A biochemical perspective, Scientific Reports, 7, 11035, 10.1038/s41598-017-11183-3, 2017.

660   McKay, N. P., Kaufman, D. S., Routson, C. C., Erb, M. P., and Zander, P. D.: The Onset and Rate of Holocene Neoglacial Cooling in the Arctic, Geophys. Res. Lett., 0, 10.1029/2018GL079773, 2018.

Melles, M., Brigham-Grette, J., Glushkova, O. Y., Minyuk, P. S., Nowaczyk, N. R., and Hubberten, H. W.: Sedimentary geochemistry of core PG1351 from Lake El'gygytgyn - a sensitive record of climate variability in the East Siberian Arctic during the past three glacial-interglacial cycles, J. Paleolimnol., 37, 89-104, 10.1007/s10933-006-9025-6, 2007.

665   Mendonça, R., Müller, R. A., Clow, D., Verpoorter, C., Raymond, P., Tranvik, L. J., and Sobek, S.: Organic carbon burial in global lakes and reservoirs, Nat. Commun., 8, 1694, 10.1038/s41467-017-01789-6, 2017.

Menne, M. J., Durre, I., Korzeniewski, B., McNeal, S., Thomas, K., Yin, X., Anthony, S., Ray, R., Vose, R. S., and Gleason, B. E.: Global historical climatology network-daily (GHCN-Daily), Version 3, NOAA National Climatic Data Center, 10, V5D21VHZ, 2012.

670   Meyer, H., Opel, T., Laepple, T., Dereviagin, A. Y., Hoffmann, K., and Werner, M.: Long-term winter warming trend in the Siberian Arctic during the mid- to late Holocene, Nat. Geosci., 8, 122-125, 10.1038/ngeo2349 http://www.nature.com/ngeo/journal/v8/n2/abs/ngeo2349.html#supplementary-information, 2015.

Meyer, H., Kostrova, S. S., Meister, P., Lenz, M. M., Kuhn, G., Nazarova, L., Syrykh, L. S., and Dvornikov, Y.: Lacustrine diatom oxygen isotopes as palaeo precipitation proxy - Holocene environmental and snowmelt variations recorded at Lake
675   Bolshoye Shchuchye, Polar Urals, Russia, Quat. Sci. Rev., 290, 107620, https://doi.org/10.1016/j.quascirev.2022.107620, 2022.

Meyers, P. A. and Teranes, J. L.: Sediment organic matter, in: Tracking Environmental Change using Lake Sediments. Volume 2: Physical and Geochemical Methods, edited by: Last, W. M., and Smol, J. P., Kluwer Academic Publisher, Dordrecht, 239-269, 2002.

680   Nazarova, L. B., Frolova, L. A., Palagushkina, O. V., Rudaya, N. A., Syrykh, L. S., Grekov, I. M., Solovieva, N., and Loskutova, O. A.: Recent shift in biological communities: A case study from the Eastern European Russian Arctic (Bol`shezemelskaya Tundra), Polar Biol., 44, 1107-1125, 10.1007/s00300-021-02876-7, 2021.

Nolan, M., Liston, G., Prokein, P., Brigham-Grette, J., Sharpton, V. L., and Huntzinger, R.: Analysis of lake ice dynamics and morphology on Lake El'gygytgyn, NE Siberia, using synthetic aperture radar (SAR) and Landsat, Journal of Geophysical
685   Research: Atmospheres, 107, ALT 3-1-ALT 3-12, https://doi.org/10.1029/2001JD000934, 2002.

Obase, T. and Abe-Ouchi, A.: Abrupt Bølling-Allerød Warming Simulated under Gradual Forcing of the Last Deglaciation, Geophys. Res. Lett., 46, 11397-11405, https://doi.org/10.1029/2019GL084675, 2019.

Oksanen, J., Blanchet, F. G., Friendly, M., Kindt, R., Legendre, P., McGlinn, D., Minchin, P. R., O'Hara, R., Simpson, G., Solymos, P., Stevens, M. H. H., Szoecs, E., and Wagner, H.: vegan: Community Ecology Package. R package version 2.5-7,
690   2020.

Pahl-Wostl, C.: Self-Regulation of Limnetic Ecosystems, in: The Lakes Handbook, 583-608, https://doi.org/10.1002/9780470999271.ch17, 2003.

Palagushkina, O., Wetterich, S., Biskaborn, B. K., Nazarova, L., Schirrmeister, L., Lenz, J., Schwamborn, G., and Grosse, G.: Diatom records and tephra mineralogy in pingo deposits of Seward Peninsula, Alaska, Palaeogeogr., Palaeoclimatol.,
695   Palaeoecol., 479, 1-15, 2017.

Palagushkina, O. V., Nazarova, L. B., Wetterich, S., and Schirrmeister, L.: Diatoms of modern bottom sediments in Siberian arctic, Contemporary Problems of Ecology, 5, 413-422, 10.1134/s1995425512040105, 2012.

Paull, T. M., Finkelstein, S. A., and Gajewski, K.: Interactions between climate and landscape drive Holocene ecological change in a High Arctic lake on Somerset Island, Nunavut, Canada, Arctic Science, 3, 17-38, 10.1139/as-2016-0013, 2017.

700   Pestryakova, L. A., Herzschuh, U., Gorodnichev, R., and Wetterich, S.: The sensitivity of diatom taxa from Yakutian lakes (north-eastern Siberia) to electrical conductivity and other environmental variables, Polar Res., 37, 10.1080/17518369.2018.1485625, 2018.

Pfalz, G., Diekmann, B., Freytag, J. C., Syrykh, L., Subetto, D. A., and Biskaborn, B. K.: Improving age–depth relationships by using the LANDO ("Linked age and depth modeling") model ensemble, Geochronology, 4, 269-295, 10.5194/gchron-4-
705   269-2022, 2022.

R Core Team: R: A language and environment for statistical computing, 2016.

Reimer, P. J., Austin, W. E. N., Bard, E., Bayliss, A., Blackwell, P. G., Bronk Ramsey, C., Butzin, M., Cheng, H., Edwards, R. L., Friedrich, M., Grootes, P. M., Guilderson, T. P., Hajdas, I., Heaton, T. J., Hogg, A. G., Hughen, K. A., Kromer, B., Manning, S. W., Muscheler, R., Palmer, J. G., Pearson, C., van der Plicht, J., Reimer, R. W., Richards, D. A., Scott, E. M.,
710   Southon, J. R., Turney, C. S. M., Wacker, L., Adolphi, F., Büntgen, U., Capano, M., Fahrni, S. M., Fogtmann-Schulz, A., Friedrich, R., Köhler, P., Kudsk, S., Miyake, F., Olsen, J., Reinig, F., Sakamoto, M., Sookdeo, A., and Talamo, S.: The IntCal20 Northern Hemisphere Radiocarbon Age Calibration Curve (0–55 cal kBP), Radiocarbon, 62, 725-757, 10.1017/RDC.2020.41, 2020.

715   Renssen, H., Seppä, H., Crosta, X., Goosse, H., and Roche, D. M.: Global characterization of the Holocene Thermal Maximum, Quat. Sci. Rev., 48, 7-19, 10.1016/j.quascirev.2012.05.022, 2012.

Rouillard, A., Michelutti, N., Rosén, P., Douglas, M. S. V., and Smol, J. P.: Using paleolimnology to track Holocene climate fluctuations and aquatic ontogeny in poorly buffered High Arctic lakes, Palaeogeogr., Palaeoclimatol., Palaeoecol., 321–322, 1-15, 10.1016/j.palaeo.2012.01.011, 2012.

Rühland, K., Paterson, A. M., and Smol, J. P.: Hemispheric-scale patterns of climate-related shifts in planktonic diatoms from
720   North American and European lakes, Global Change Biol., 14, 2740-2754, 10.1111/j.1365-2486.2008.01670.x, 2008.

Rühland, K. M., Paterson, A. M., and Smol, J. P.: Lake diatom responses to warming: reviewing the evidence, J. Paleolimnol., 54, 1-35, DOI: 10.1007/s10933-015-9837-3, 2015.

Rutkowski, C., Lenz, J., Lang, A., Wolter, J., Mothes, S., Reemtsma, T., Grosse, G., Ulrich, M., Fuchs, M., Schirrmeister, L., Fedorov, A., Grigoriev, M., Lantuit, H., and Strauss, J.: Mercury in Sediment Core Samples From Deep Siberian Ice-Rich
725   Permafrost, Frontiers in Earth Science, 9, 10.3389/feart.2021.718153, 2021.

Ryves, D., Juggins, S., Fritz, S., and Battarbee, R.: Experimental diatom dissolution and the quantification of microfossil preservation in sediments, Palaeogeog. Palaeoclimatol. Palaeoecol., 172, 99-113, 2001.

Sadler, P. M.: Sediment Accumulation Rates and the Completeness of Stratigraphic Sections, The Journal of Geology, 89, 569-584, 10.1086/628623, 1981.

730 Scussolini, P., Vegas-Vilarrúbia, T., Rull, V., Corella, J. P., Valero-Garcés, B., and Goma, J.: Middle and late Holocene climate change and human impact inferred from diatoms, algae and aquatic macrophyte pollen in sediments from Lake Montcortès (NE Iberian Peninsula), J. Paleolimnol., 46, 369-385, 2011.

Shevtsova, I., Heim, B., Kruse, S., Schröder, J., Troeva, E. I., Pestryakova, L. A., Zakharov, E. S., and Herzschuh, U.: Strong shrub expansion in tundra-taiga, tree infilling in taiga and stable tundra in central Chukotka (north-eastern Siberia) between 735 2000 and 2017, Environmental Research Letters, 15, 085006, 10.1088/1748-9326/ab9059, 2020.

Smol, J. P. and Stoermer, E. F.: The Diatoms: Applications for the Environmental and Earth Sciences, 2, Cambridge Univ Pr, 667 pp.2010.

Smol, J. P., Wolfe, A. P., Birks, H. J. B., Douglas, M. S. V., Jones, V. J., Korhola, A., Pienitz, R., Rühland, K., Sorvari, S., Antoniades, D., Brooks, S. J., Fallu, M. A., Hughes, M., Keatley, B. E., Laing, T. E., Michelutti, N., Nazarova, L., Nyman, M., 740 Paterson, A. M., Perren, B., Quinlan, R., Rautio, M., Saulnier-Talbot, E., Siitoneni, S., Solovieva, N., and Weckstrom, J.: Climate-driven regime shifts in the biological communities of arctic lakes, Proc. Natl. Acad. Sci. USA, 102, 4397-4402, 10.1073/pnas.0500245102, 2005.

Sobek, S., Durisch-Kaiser, E., Zurbrügg, R., Wongfun, N., Wessels, M., Pasche, N., and Wehrli, B.: Organic carbon burial efficiency in lake sediments controlled by oxygen exposure time and sediment source, Limnol. Oceanogr., 54, 2243-2254, 745 https://doi.org/10.4319/lo.2009.54.6.2243, 2009.

Subetto, D. A., Nazarova, L. B., Pestryakova, L. A., Syrykh, L. S., Andronikov, A. V., Biskaborn, B., Diekmann, B., Kuznetsov, D. D., Sapelko, T. V., and Grekov, I. M.: Paleolimnological studies in Russian northern Eurasia: A review, Contemporary Problems of Ecology, 10, 327-335, 10.1134/s1995425517040102, 2017.

Sundqvist, H. S., Kaufman, D. S., McKay, N. P., Balascio, N. L., Briner, J. P., Cwynar, L. C., Sejrup, H. P., Seppa, H., Subetto, 750 D. A., Andrews, J. T., Axford, Y., Bakke, J., Birks, H. J. B., Brooks, S. J., de Vernal, A., Jennings, A. E., Ljungqvist, F. C., Ruehland, K. M., Saenger, C., Smol, J. P., and Viau, A. E.: Arctic Holocene proxy climate database - new approaches to assessing geochronological accuracy and encoding climate variables, Climate of the Past, 10, 1605-1631, 10.5194/cp-10-1605-2014, 2014.

Swann, G. E. A., Leng, M. J., Juschus, O., Melles, M., Brigham-Grette, J., and Sloane, H. J.: A combined oxygen and silicon 755 diatom isotope record of Late Quaternary change in Lake El'gygytgyn, North East Siberia, Quat. Sci. Rev., 29, 774-786, https://doi.org/10.1016/j.quascirev.2009.11.024, 2010.

Syvitski, J., Waters, C. N., Day, J., Milliman, J. D., Summerhayes, C., Steffen, W., Zalasiewicz, J., Cearreta, A., Gałuszka, A., Hajdas, I., Head, M. J., Leinfelder, R., McNeill, J. R., Poirier, C., Rose, N. L., Shotyk, W., Wagreich, M., and Williams, M.: Extraordinary human energy consumption and resultant geological impacts beginning around 1950 CE initiated the proposed 760 Anthropocene Epoch, Communications Earth & Environment, 1, 32, 10.1038/s43247-020-00029-y, 2020.

Valiranta, M., Weckstrom, J., Siitonen, S., Seppa, H., Alkio, J., Juutinen, S., and Tuittila, E. S.: Holocene aquatic ecosystem change in the boreal vegetation zone of northern Finland, J. Paleolimnol., 45, 339-352, 10.1007/s10933-011-9501-5, 2011.

Virtanen, P., Gommers, R., Oliphant, T. E., Haberland, M., Reddy, T., Cournapeau, D., Burovski, E., Peterson, P., Weckesser, W., Bright, J., van der Walt, S. J., Brett, M., Wilson, J., Millman, K. J., Mayorov, N., Nelson, A. R. J., Jones, E., Kern, R., 765 Larson, E., Carey, C. J., Polat, İ., Feng, Y., Moore, E. W., VanderPlas, J., Laxalde, D., Perktold, J., Cimrman, R., Henriksen, I., Quintero, E. A., Harris, C. R., Archibald, A. M., Ribeiro, A. H., Pedregosa, F., van Mulbregt, P., Vijaykumar, A., Bardelli, A. P., Rothberg, A., Hilboll, A., Kloeckner, A., Scopatz, A., Lee, A., Rokem, A., Woods, C. N., Fulton, C., Masson, C., Häggström, C., Fitzgerald, C., Nicholson, D. A., Hagen, D. R., Pasechnik, D. V., Olivetti, E., Martin, E., Wieser, E., Silva, F., Lenders, F., Wilhelm, F., Young, G., Price, G. A., Ingold, G.-L., Allen, G. E., Lee, G. R., Audren, H., Probst, I., Dietrich, J. 770 P., Silterra, J., Webber, J. T., Slavič, J., Nothman, J., Buchner, J., Kulick, J., Schönberger, J. L., de Miranda Cardoso, J. V., Reimer, J., Harrington, J., Rodríguez, J. L. C., Nunez-Iglesias, J., Kuczynski, J., Tritz, K., Thoma, M., Newville, M., Kümmerer, M., Bolingbroke, M., Tartre, M., Pak, M., Smith, N. J., Nowaczyk, N., Shebanov, N., Pavlyk, O., Brodtkorb, P. A., Lee, P., McGibbon, R. T., Feldbauer, R., Lewis, S., Tygier, S., Sievert, S., Vigna, S., Peterson, S., More, S., Pudlik, T., Oshima, T., Pingel, T. J., Robitaille, T. P., Spura, T., Jones, T. R., Cera, T., Leslie, T., Zito, T., Krauss, T., Upadhyay, U., 775 Halchenko, Y. O., Vázquez-Baeza, Y., and SciPy, C.: SciPy 1.0: fundamental algorithms for scientific computing in Python, Nat. Methods, 17, 261-272, 10.1038/s41592-019-0686-2, 2020.

Vyse, S. A., Herzschuh, U., Andreev, A. A., Pestryakova, L. A., Diekmann, B., Armitage, S. J., and Biskaborn, B. K.: Geochemical and sedimentological responses of arctic glacial Lake Ilirney, chukotka (far east Russia) to palaeoenvironmental change since ~51.8 ka BP, Quat. Sci. Rev., 247, 106607, https://doi.org/10.1016/j.quascirev.2020.106607, 2020.

780   Vyse, S. A., Herzschuh, U., Pfalz, G., Pestryakova, L. A., Diekmann, B., Nowaczyk, N., and Biskaborn, B. K.: Sediment and carbon accumulation in a glacial lake in Chukotka (Arctic Siberia) during the Late Pleistocene and Holocene: combining hydroacoustic profiling and down-core analyses, Biogeosciences, 18, 4791-4816, 10.5194/bg-18-4791-2021, 2021.

Wilson, C. R., Michelutti, N., Cooke, C. A., Briner, J. P., Wolfe, A. P., and Smol, J. P.: Arctic lake ontogeny across multiple interglaciations, Quat. Sci. Rev., 31, 112-126, 10.1016/j.quascirev.2011.10.018, 2012.

785   Wohlfarth, B., Lacourse, T., Bennike, O., Subetto, D., Tarasov, P., Demidov, I., Filimonova, L., and Sapelko, T.: Climatic and environmental changes in north-western Russia between 15,000 and 8000calyrBP: a review, Quat. Sci. Rev., 26, 1871-1883, https://doi.org/10.1016/j.quascirev.2007.04.005, 2007.

Wolfe, A. P.: On diatom concentrations in lake sediments: results from an inter-laboratory comparison and other tests performed on a uniform sample, J. Paleolimnol., 18, 261-268, 1997.

790   Wunsam, S., Schmidt, R., and Klee, R.: Cyclotella-taxa (Bacillariophyceae) in lakes of the Alpine region and their relationship to environmental variables, Aquat. Sci., 57, 360-386, 1995.

Yoon, J. E., Yoo, K. C., Macdonald, A. M., Yoon, H. I., Park, K. T., Yang, E. J., Kim, H. C., Lee, J. I., Lee, M. K., Jung, J., Park, J., Lee, J., Kim, S., Kim, S. S., Kim, K., and Kim, I. N.: Reviews and syntheses: Ocean iron fertilization experiments – past, present, and future looking to a future Korean Iron Fertilization Experiment in the Southern Ocean (KIFES) project, 795   Biogeosciences, 15, 5847-5889, 10.5194/bg-15-5847-2018, 2018.

Zhuravlev, G., Kazymin, S., and Pukalo, P.: State geological map of the Russian Federation, scale 1: 200 000, Anjuyjsker-Chaunsker Series, Moscow, St, 1999.
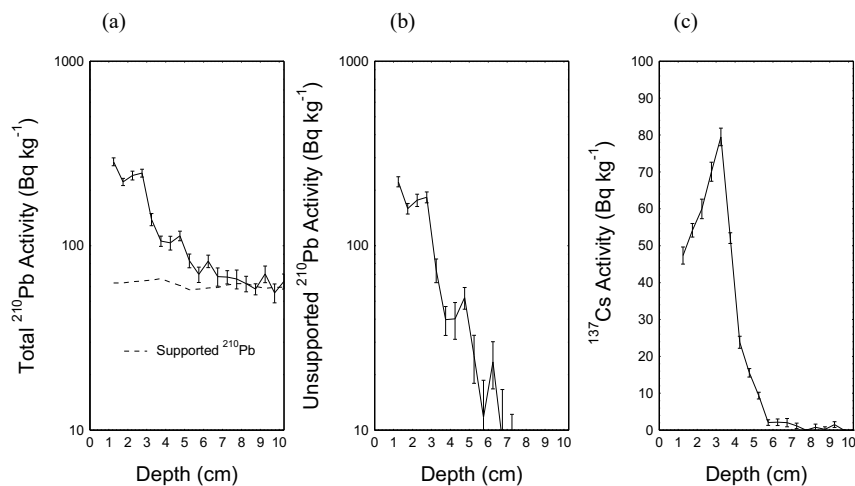
800

Figures and Tables
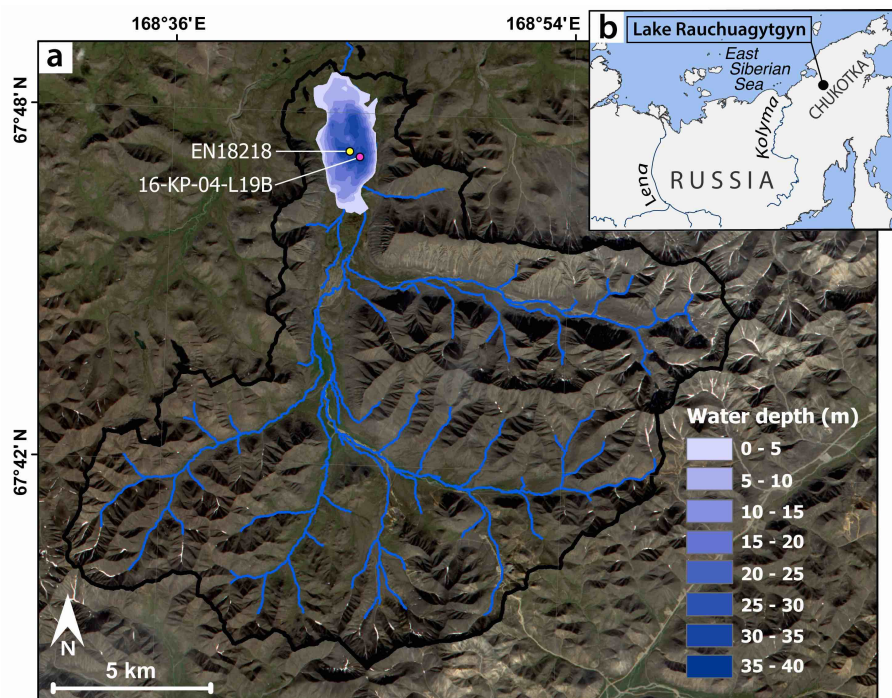
Figure 1: Study site. a, bathymetrical map of Lake Rauchuagytgyn with catchment area (boundary as
805 **black line, inflows as blue lines,) and coring locations (long core EN18218; short core 16-KP-04-L19B). b,**
**geographical overview map. Map based on ESRI (Esri and Geoeye, 2019).**

810 **Figure 2: Fallout radionuclides in short core 16-KP-04-L19B showing (a) total and supported ^{210}Pb, (b)**
**unsupported ^{210}Pb, (c) ^{137}Cs concentrations versus depth.**
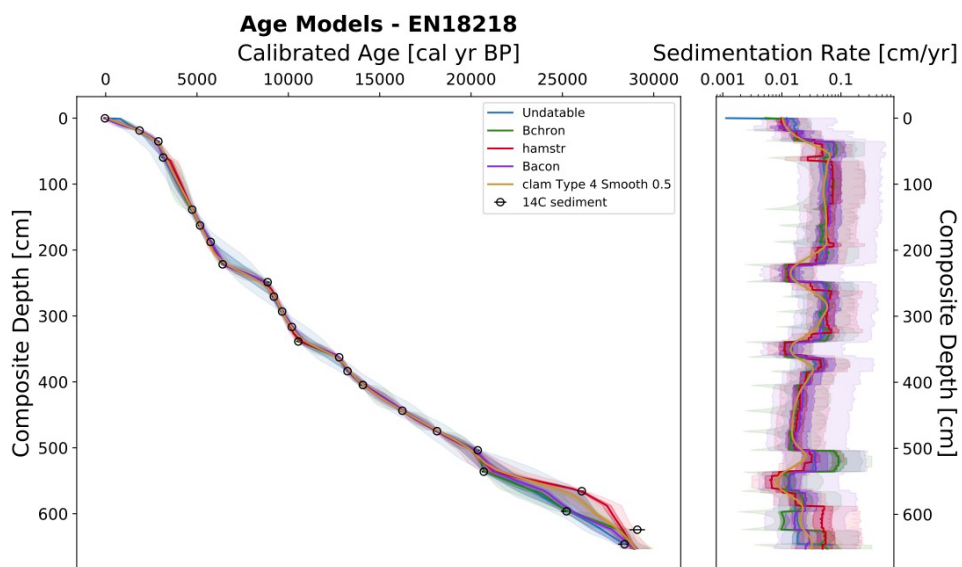
Figure 3: Generated output from LANDO for sediment core EN18218 based on ^{14}C data from Vyse et al. (2021). Left plot consists of a comparison between five age-depth models from different modelling codes indicated in the legend. Colored solid lines indicate the median age, while shaded areas represent their respective 1σ and 2σ ranges in the same colors with decreasing opacities. Right plot shows the calculated sedimentation rate with matching colors. Black circles in the left plot indicate the mean calibrated ages of ^{14}C bulk sediment samples based on IntCal20 calibration curve (Reimer et al., 2020) and their 1σ uncertainty error bars.
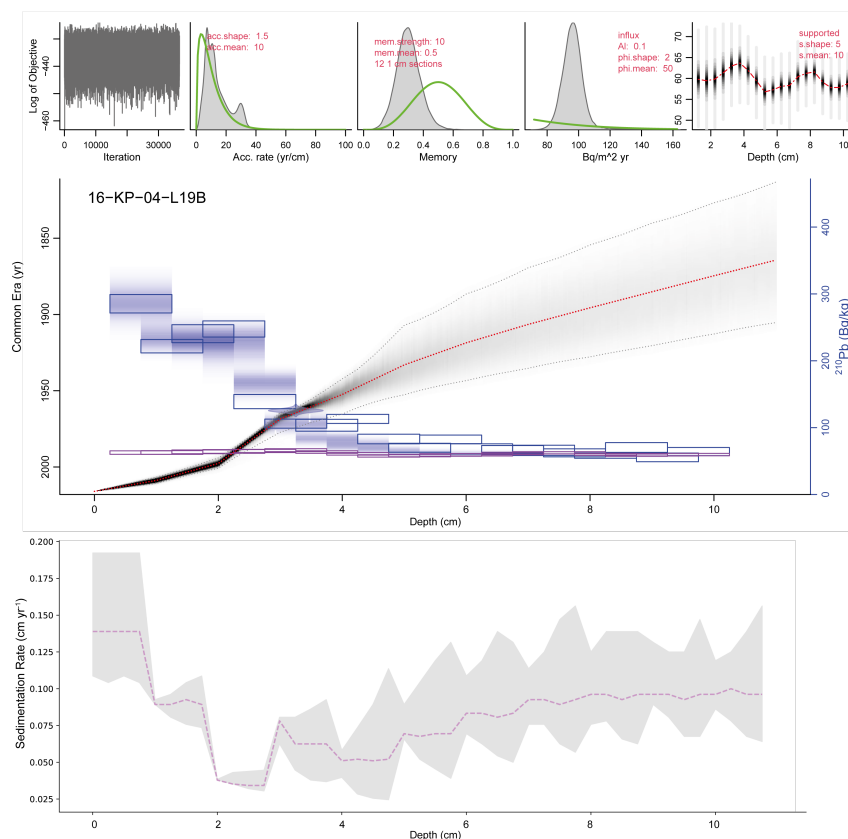
Figure 4: Plum age-depth model for sediment core 16-KP-04-L19B. The five upper panels show the Bayesian input parameters and their posterior distributions for Plum. The middle panel consists of the age-depth model with its mean age in red and its 2σ confidence interval in grey, the unsupported ^{210}Pb concentrations (in Bq/kg) in blue with its 1σ uncertainty, and the supported ^{210}Pb concentrations (in Bq/kg) in violet. The lower panel displays the mean sedimentation rate over depth as dashed line and the 2σ confidence interval in grey.
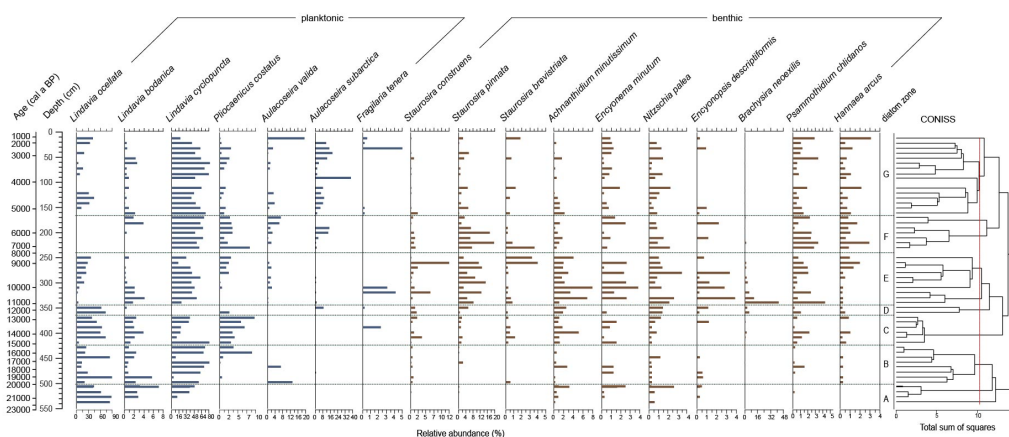
Figure 5: Relative abundance of diatom species in the long core EN18218. Diatom zones established by CONISS clustering. Species % values are shown next to the mean calibrated ages before present and the core depth below the sediment surface. Taxa present with ≥ 3% in ≥ 2 samples were included in the graph.

835
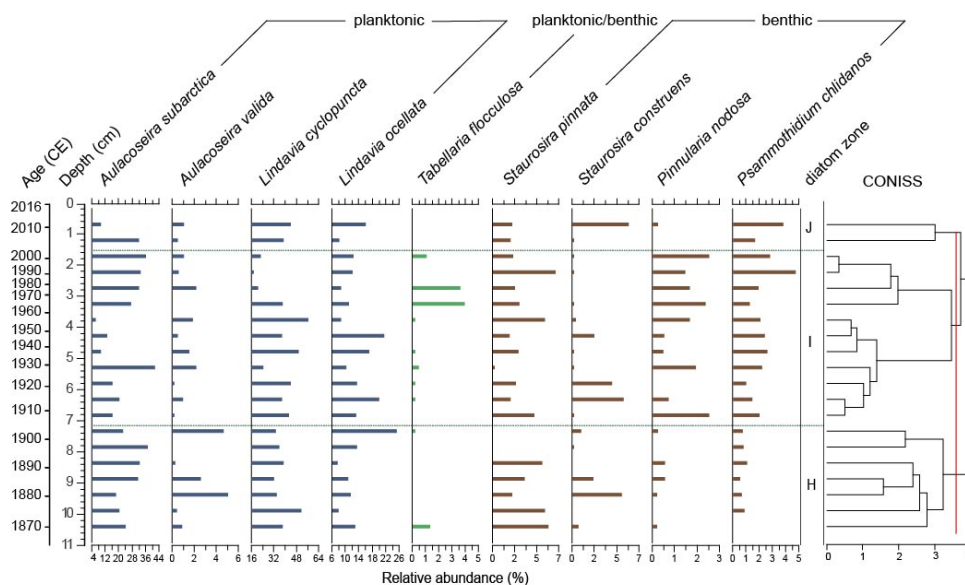
Figure 6: Relative abundance of diatom species in the short core 16-KP-04-L19B. Diatom zones established by CONISS clustering. Species % values are shown next to calibrated mean ages (common era years, CE) and the core depth below sediment surface. Taxa present with ≥ 3% in ≥ 2 samples were included in the graph.

840
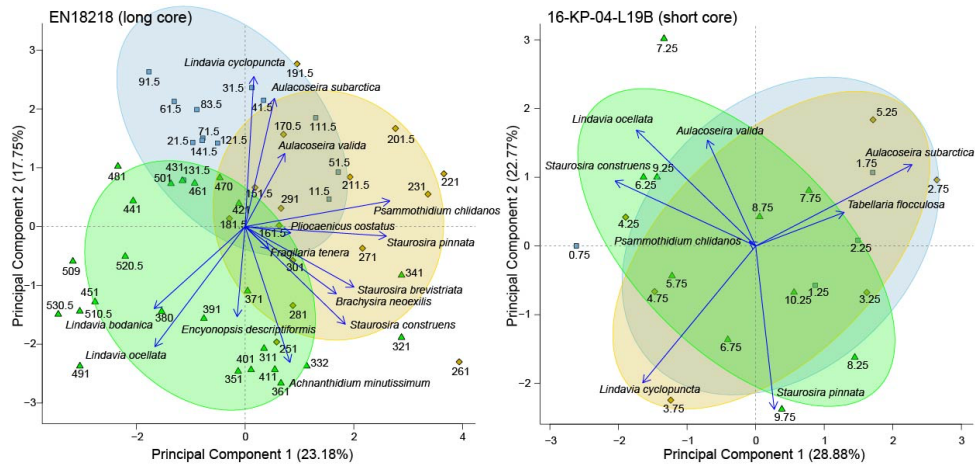
Figure 7: Biplots of the first two dimensions (PC1, PC2) generated by principal component analysis of diatom species filtered to ≥ 3% in ≥ 2 samples from long core EN18218 and short core 16-KP-04-L19B. Color circles represent eco-taxonomical clusters with comparable environmental preferences. Explained variance of each PC is indicated at the axis label in %.
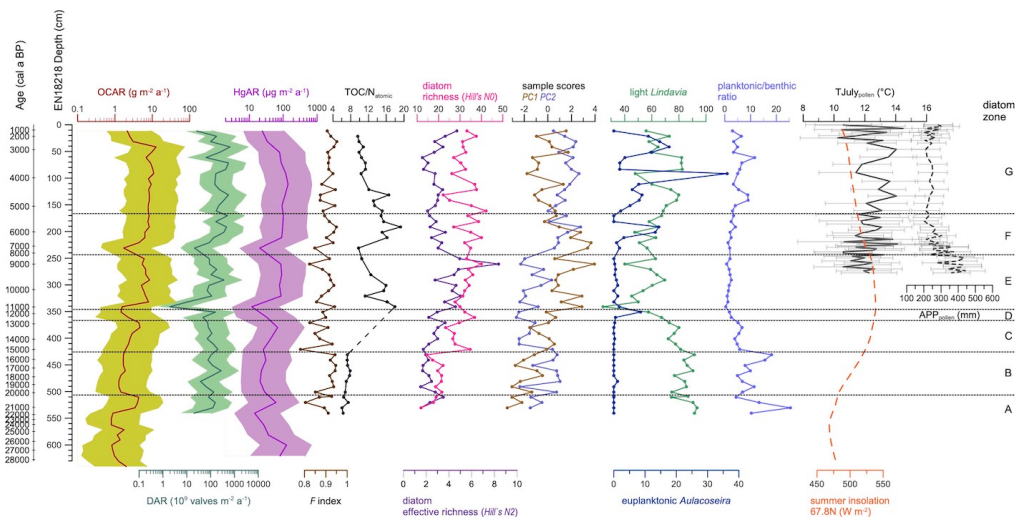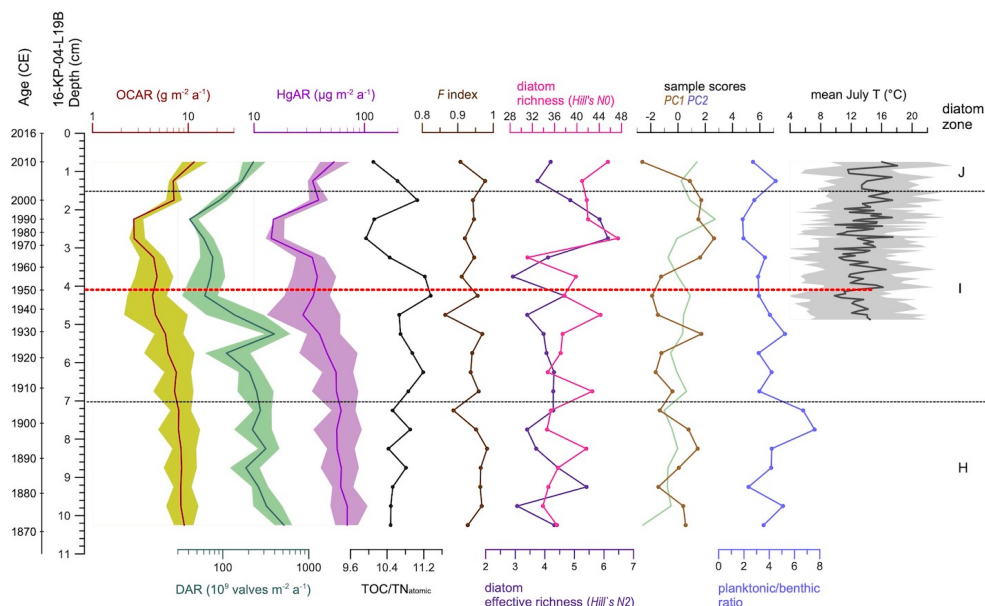

Figure 8: Biogeochemical variables and statistical diatom indices since the Late Pleistocene from Lake Rauchuagytgyn sediment core EN18218. OCAR, organic carbon accumulation rates; DAR, diatom accumulation rates; HgAR, mercury accumulation rates; *F* index, diatom valve preservation index; TOC/TN_atomic, total organic carbon to total nitrogen ratio; diatom species richness based on Hill numbers; PC1-3, main axes sample scores from the principal component analysis; light 'cyclotelloid' *Lindavia* and euplanktonic *Aulacoseira* as sum percentages; planktonic to benthic species ratios; paleoclimate information from published literature at the right. Reconstructed July temperatures and precipitation

adopted from Andreev et al. (2021), OCAR and TOC/TN$_{atomic}$ is based on organic carbon concentrations from Vyse et al. (2021), insolation is based on orbital parameters from Laskar et al. (2004).

860

Figure 9: Biogeochemical variables and statistical diatom indices over the last decades from Lake Rauchuagytgyn surface sediment core 16-KP-04-L19B. OCAR, organic carbon accumulation rates; DAR, diatom accumulation rates; HgAR, mercury accumulation rates; TOC/TN$_{atomic}$, total organic carbon to nitrogen ratio; *F* index, diatom valve preservation index; diatom species richness based on Hill numbers; PC1-3, main axes sample scores from the principal component analysis; planktonic to benthic species ratios; July temperatures (mean, min, max) calculated from OSTROVNOE weather station (www.noaa.gov). Red dotted line indicates T increase and onset of the Anthropocene

865
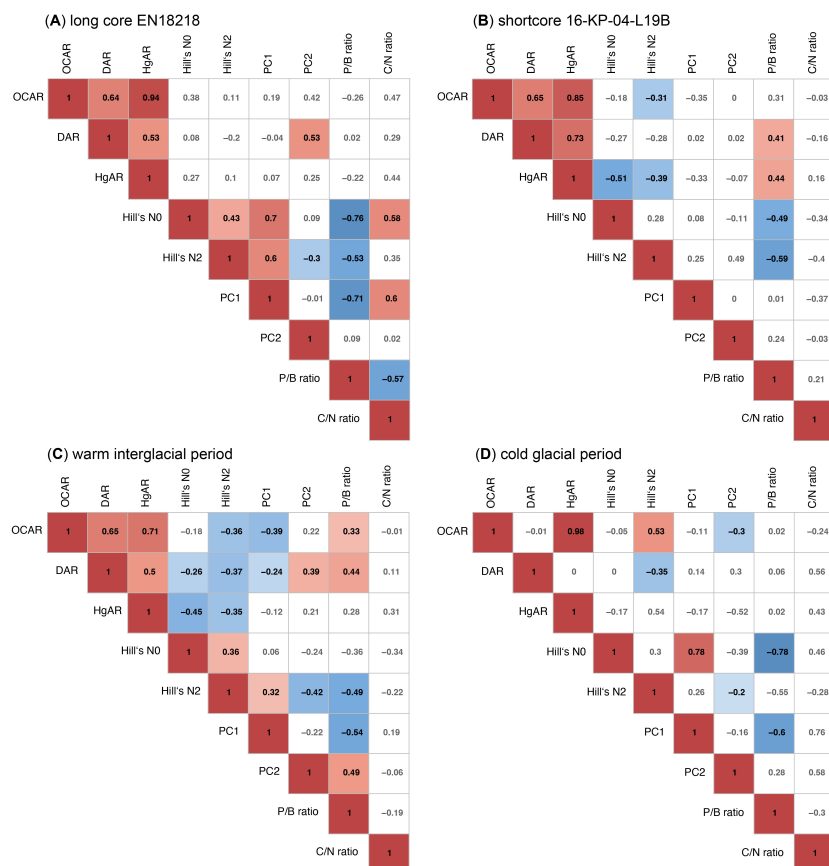
870

Figure 10: Pearson correlation matrix between organic matter, diatom indices, and mercury variables. Red, positive correlations; blue, negative correlations. p values correction of <0.05 was applied to assign colors only to significant correlations. Insignificant correlations shown as grey numbers within white cells. Panels A and B represent correlations within the individual core records. Panels B and C represent correlations in the warm period including the short core and the Holocene part of core EN18218 (C), and the cold period restricted to the pre-Holocene part of core EN18218 (D).
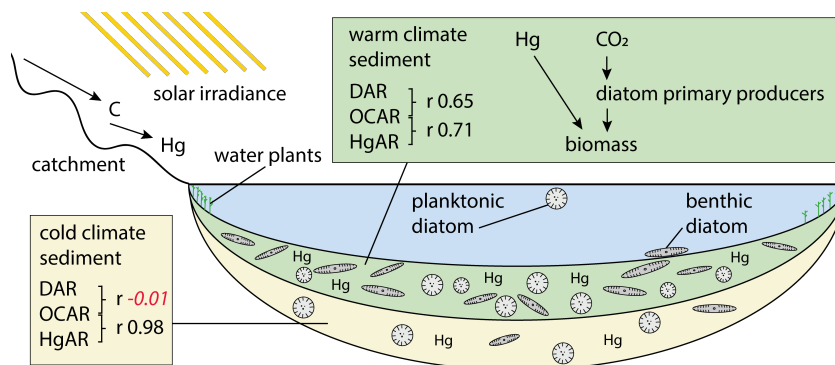
880   **Figure 11: Schematic drawing of the long-term processes leading to accumulation of diatom valves (DAR), organic carbon (OCAR), and mercury (HgAR) in Lake Rauchuagytgyn. Pearson correlation coefficients indicated by r in black when correlation was significant (p<0.05), and in red italic when p>0.05 (insignificant).**

885

Table 1: Radiocarbon dates from sediment core EN18218 from Vyse et al. (2021) used to generate age-depth relationships and sedimentation rates in LANDO.

Lab code	Sample ID	Composite depth (cm)	Radiocarbon age with error (^{14}C years BP)	Sample type
AWI - 5627.1.1	EN18218-1 Surface 0-0.5 cm	0.25	785 ± 31	Bulk, TOC
AWI - 2998.1.1	EN18218-2_0-100_20-20.5	18.75	2787 ± 33	Bulk, TOC
AWI - 2999.1.1	EN18218-2_0-100_36.5-37	35.25	3629 ± 33	Bulk, TOC
AWI - 3000.1.1	EN18218-2_0-100_61-61.5	59.75	3832 ± 33	Bulk, TOC
AWI - 3003.1.1	EN18218-2_100-200_140-140.5	138.75	5074 ± 34	Bulk, TOC
AWI - 3004.1.1	EN18218-2_100-200_164-164.5	162.75	5382 ± 34	Bulk, TOC
AWI - 3005.1.1	EN18218-2_100-200_189-189.5	187.75	5852 ± 34	Bulk, TOC
AWI - 3006.1.1	EN18218-2_200-240_222.5-223	221.75	6472 ± 35	Bulk, TOC
AWI - 3007.1.2	EN18218-3_0-100_15-15.5	248.75	8872 ± 37	Bulk, TOC
AWI - 3008.1.1	EN18218-3_0-100_37-37.5	270.75	9085 ± 37	Bulk, TOC
AWI - 3009.1.1	EN18218-3_0-100_59.5-60	293.25	9516 ± 38	Bulk, TOC
AWI - 3010.1.1	EN18218-3_0-100_83-83.5	316.75	9901 ± 39	Bulk, TOC
AWI - 3011.1.1	EN18218-3_100-200_105-105.5	338.75	10197 ± 39	Bulk, TOC
AWI - 3012.11	EN18218-3_100-200_129-129.5	362.75	11687 ± 30	Bulk, TOC
AWI - 3013.1.1	EN18218-3_100-200_150-150.5	383.75	12205 ± 46	Bulk, TOC
AWI - 3014.1.1	EN18218-3_100-200_171-171.5	404.75	13017 ± 48	Bulk, TOC
AWI - 3015.1.1	EN18218-3_200-292_210-210.5	443.75	14330 ± 52	Bulk, TOC
AWI - 3016.1.1	EN18218-3_200-292_239-239.5	474.75	15686 ± 48	Bulk, TOC

AWI - 3017.1.1	EN18218-3_200-292_270-270.5	503.75	17708 ± 56	Bulk, TOC
AWI - 3018.1.1	EN18218-4_0-100_35-35.5	536.25	18000 ± 55	Bulk, TOC
AWI - 3019.1.1	EN18218-4_0-100_64.5-65	565.75	22649 ± 66	Bulk, TOC
AWI - 3020.1.1	EN18218-4_0-100_95-95.5	596.25	21786 ± 204	Bulk, TOC
AWI - 3021.1.1	EN18218-4_100-163_123-123.5	624.25	25689 ± 325	Bulk, TOC
AWI - 3022.1.1	EN18218-4_100-163_145-145.5	646.25	25081 ± 300	Bulk, TOC

890 **Table 2: Fallout radionuclide concentrations in the short core 16-KP-04-L19B**

| Depth | | ^{210}Pb | | | | | | ^{137}Cs | |
| | | Total | | Unsupported | | Supported | | | |
cm	g cm^{-2}	Bq kg^{-1}	±	Bq kg^{-1}	±	Bq kg^{-1}	±	Bq kg^{-1}	±
1.25	0.29	285.3	13.8	222.5	14.1	62.7	2.6	47.3	2.3
1.75	0.40	221.8	10.0	159.0	10.4	62.8	2.8	54.2	1.8
2.25	0.52	240.5	13.4	176.6	13.6	63.8	2.8	60.0	2.6
2.75	0.62	247.6	12.1	183.1	12.4	64.4	2.8	70.1	2.6
3.25	0.75	138.9	10.6	73.8	10.8	65.1	2.4	79.5	2.4
3.75	0.94	106.0	6.8	39.7	7.1	66.3	2.2	52.1	1.4
4.25	1.15	103.6	8.9	40.1	9.1	63.5	1.9	23.8	1.6
4.75	1.34	113.1	6.8	52.3	7.1	60.8	1.9	15.6	1.2
5.25	1.54	83.0	7.2	25.3	7.4	57.7	1.8	9.4	0.9
5.75	1.75	69.9	6.7	11.7	6.9	58.2	1.8	2.1	0.8
6.25	1.93	82.5	6.4	23.4	6.7	59.1	1.9	2.2	0.9
6.75	2.11	68.1	7.7	8.7	7.9	59.4	1.8	2.0	1.1
7.25	2.31	67.6	5.6	6.3	5.9	61.3	1.9	1.2	0.7
7.75	2.51	66.0	7.7	3.7	7.9	62.3	1.7	0.0	0.0
8.25	2.71	62.3	6.0	-0.2	6.2	62.4	1.6	0.8	0.9
8.75	2.91	58.2	4.0	-1.9	4.3	60.0	1.6	0.2	0.7
9.25	3.12	70.3	7.3	11.5	7.5	58.8	1.7	1.5	0.8
9.75	3.32	55.5	6.5	-4.0	6.8	59.5	1.9	0.0	0.0
10.25	3.53	64.2	6.1	4.6	6.3	59.7	1.8	0.0	0.0